Observational Analysis of the Predictability of Mesoscale Convective Systems

ISRAEL L. JIRAK AND WILLIAM R. COTTON

Department of Atmospheric Science, Colorado State University, Fort Collins, Colorado

(Manuscript received 30 December 2005, in final form 4 October 2006)

ABSTRACT

Mesoscale convective systems (MCSs) have a large influence on the weather over the central United States during the warm season by generating essential rainfall and severe weather. To gain insight into the predictability of these systems, the precursor environments of several hundred MCSs across the United States were reviewed during the warm seasons of 1996–98. Surface analyses were used to identify initiating mechanisms for each system, and North American Regional Reanalysis (NARR) data were used to examine the environment prior to MCS development. Similarly, environments unable to support organized convective systems were also investigated for comparison with MCS precursor environments. Significant differences were found between environments that support MCS development and those that do not support convective organization. MCSs were most commonly initiated by frontal boundaries; however, features that enhance convective initiation are often not sufficient for MCS development, as the environment needs also to be supportive for the development and organization of long-lived convective systems. Low-level warm air advection, low-level vertical wind shear, and convective instability were found to be the most important parameters in determining whether concentrated convection would undergo upscale growth into an MCS. Based on these results, an index was developed for use in forecasting MCSs. The MCS index assigns a likelihood of MCS development based on three terms: 700-hPa temperature advection, 0–3-km vertical wind shear, and the lifted index. An evaluation of the MCS index revealed that it exhibits features consistent with common MCS characteristics and is reasonably accurate in forecasting MCSs, especially given that convective initiation has occurred, offering the possibility of usefulness in operational forecasting.

1. Introduction

Mesoscale convective systems (MCSs) frequently develop and traverse the central United States during the warm season. The prediction of these common, large thunderstorm complexes is important for two contrasting reasons. On the positive side, they generate essential rainfall for this agricultural region (Fritsch et al. 1986; Jirak et al. 2003; Ashley et al. 2003) while, on the negative side, they devastate property and possessions by producing severe weather (e.g., hail, damaging winds, flash floods, and tornadoes) over a large area (Maddox 1980; Houze et al. 1990; Jirak et al. 2003). Regardless of whether the impact of MCSs is primarily beneficial or harmful, advance knowledge of their development is desirable.

Unfortunately, forecasting MCSs is not only very challenging, but it is also an area with an overall lack of knowledge and specific prediction methods (Ziegler 2000). MCSs develop from individual thunderstorm cells that interact and subsequently merge into a large, long-lived organized convective system (Cotton and Anthes 1989). Thus, forecasting MCSs requires knowledge of areas favorable for convective initiation, organization, and sustenance over a range of spatial and time scales. Even though pinpointing the location of convective initiation is unlikely in most cases, considerable information pertinent to forecasting can still be learned about environments that are conducive for convective organization and sustenance. In fact, mesoscale convective complexes (MCCs), a specific type of MCS (Maddox 1980), tend to form frequently only in certain regions of the world with preferred geographical settings (e.g., leeward side of the Rocky Mountains in the United States, leeward side of the Andes Mountains in South America, leeward side of the Himalayas in China, and tropical western Africa) that repeatedly

Corresponding author address: Israel L. Jirak, Dept. of Atmospheric Science, Colorado State University, Fort Collins, CO 80523.
E-mail: ijirak@atmos.colostate.edu

DOI: 10.1175/WAF1012.1

produce favorable meteorological conditions for these systems (Laing and Fritsch 1997, 2000), lending support to the possibility of improving forecasts of MCSs.

The objective of the current study is to exploit this notion of MCS predictability by identifying important MCS precursors through a detailed observational analysis of the environment prior to the development of hundreds of MCSs over the United States. This study builds on previous studies regarding the precursor environment of MCCs (Maddox 1983; Augustine and Howard 1988; Cotton et al. 1989; Laing and Fritsch 2000) and other MCSs (Augustine and Caracena 1994; Anderson and Arritt 1998) by using data of higher temporal and spatial resolution to analyze many more and varied types of MCSs with the purpose of investigating MCS predictability. To address the issue of MCS predictability in a comprehensive manner, the MCS precursor environments are compared with environments that do not support long-lived, organized convection. From the analysis of these different conditions, parameters that accurately distinguish environments favorable for MCS development are identified as possible aids in forecasting MCSs. The ultimate goal of this study is to develop an MCS index based on these parameters that can forecast accurately the likelihood of MCS development in the next few hours at a given location.

2. Background

a. Forecasting convective storms

One of the greatest forecasting challenges involves deciding if, when, and where convective initiation will occur. Even when there is a large amount of convective available potential energy (CAPE), thunderstorm development is not guaranteed. Often times, there is enough convective inhibition (CIN) to prevent thunderstorms from forming. Daytime heating, large-scale ascent, and lifting along surface boundaries are all capable of overcoming CIN, leading to thunderstorm development. Since mesoscale boundaries can provide enough lift to initiate storms, the ability to locate these features is vital in order to correctly forecast the timing and location of convective initiation. Unfortunately, the current density of the observational network is not sufficient to resolve many of the mesoscale features important to convective initiation (Stensrud and Fritsch 1994). Therefore, the issue of convective initiation is not addressed here.

However, the difficulty in forecasting thunderstorms does not end with the issue of convective initiation. Once thunderstorms develop, they can take on many different characteristics and appearances depending on the local environment. Widely recognized modes of convection include ordinary thunderstorms, multicell thunderstorms, supercell thunderstorms, and MCSs (including convective lines and clusters of all shapes and sizes). Vertical wind shear is one parameter that plays an important role in determining the mode of convection. Weisman and Klemp (1982, 1984) found that for similar values of CAPE, ordinary, multicell, and supercell thunderstorms are likely for small, intermediate, and large values of low-level shear, respectively. In accordance with this finding, thunderstorms that develop in an area with large values of shear have a high likelihood of producing severe weather (Johns and Doswell 1992; McNulty 1995). Although vertical wind shear is useful in discerning the type of convective cells that will form, it typically does not provide sufficient information in determining whether these thunderstorms will undergo upscale growth into MCSs. In fact, Doswell and Flueck (1989) and Jincai et al. (1992) reported that even though experimental forecasters were able to provide reasonably accurate forecasts of deep convection, they showed only marginal skill in determining the degree to which thunderstorms would experience mesoscale organization. Therefore, given the difficulty of forecasting MCSs combined with the scarcity of specific forecasting methods, the issue of forecasting MCSs requires more attention.

b. Precursor environment of MCSs

For just over a quarter-century, research on MCSs has significantly increased our awareness and understanding of these massive convective storms. Several studies (e.g., Maddox 1983; Augustine and Howard 1988; Cotton et al. 1989; Augustine and Caracena 1994; Anderson and Arritt 1998; Laing and Fritsch 2000) have examined the large-scale environment prior to MCS development in order to identify recurrent features of the MCS precursor environment, focusing primarily on MCCs. These studies form the current basis of MCS forecasting, and their results are summarized below.

The upper and middle levels are generally characterized by relatively weak flow prior to MCS development with systems typically developing just upstream of a broad ridge (Maddox 1983; Cotton et al. 1989; Anderson and Arritt 1998; Laing and Fritsch 2000). MCSs generally form in the right entrance region of a jet streak (Cotton et al. 1989; Anderson and Arritt 1998), where there tends to be ascent, favoring thunderstorm development (Uccellini and Johnson 1979). In the lower troposphere, more-pronounced features are found prior to MCS development, including strong warm air advection at 700 hPa (Fig. 1). As several stud-

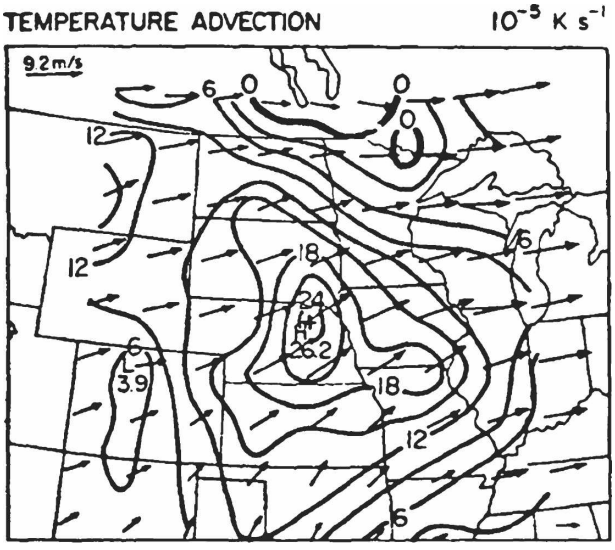

FIG. 1. Composite of 700-hPa temperature advection and wind vectors at the initial stage of MCC development. The center grid point (plus sign) denotes the average MCC position at initiation (from Cotton et al. 1989).

ies have noted (e.g., Maddox and Doswell 1982; Maddox 1983; Cotton et al. 1989; Laing and Fritsch 2000), warm air advection is often collocated with the area where MCS development occurs, suggesting that ascent associated with warm advection is helpful for the development and sustenance of MCSs. A strong, southerly low-level jet (LLJ) exists at 850 hPa advecting warm, moist air into the region of MCS development (Fig. 2) (Maddox 1983; Cotton et al. 1989; Anderson and Arritt 1998; Laing and Fritsch 2000). At the surface, convergence is commonly found along an east–west-oriented front stretching through the moist, unstable region of MCS development (Fig. 3) (Maddox 1983; Cotton et al. 1989; Anderson and Arritt 1998; Laing and Fritsch 2000). In fact, the intersection of this front and the LLJ can be a preferred region for MCS genesis, as is illustrated in Fig. 4 where the late afternoon surface geostrophic wind maximum serves as a proxy for the location of the nocturnal LLJ (Augustine and Caracena 1994).

As discussed previously, low-level vertical wind shear has an important influence on the type and severity of the thunderstorm that develops. Rotunno et al. (1988), Weisman (1992), and Weisman and Rotunno (2004) also postulate that low-level vertical wind shear is critical to sustaining long-lived squall lines through its interaction with the convectively generated cold pool. When the horizontal vorticity of the ambient shear interacts with the horizontal vorticity associated with the cold pool, deep lifting is facilitated at the leading edge of the cold pool, creating strong convective cells. Thus, the effect of low-level shear is to enhance vertical lifting at the leading edge of the storm's outflow, promoting the development of an MCS. Laing and Fritsch (2000) found that MCCs around the globe typically form near a maximum in low-level shear (see Fig. 5), lending support to the idea that low-level shear may be important for the development of long-lived MCSs.

3. Data and methodology

For this study, the geographical area under consideration is the central United States excluding only areas west of the Rocky Mountains and east of the Appalachian Mountains. The dependent study period includes the warm seasons (April–August) of 1996–98 during which 387 MCSs of all shapes and sizes were objectively identified using infrared (IR) satellite data (see Jirak et al. 2003). An independent convective period from 20 May to 6 July 2003 during the Bow Echo and Mesoscale Convective Vortex (MCV) Experiment (BAMEX) (Davis et al. 2004) was also examined for verification purposes, and an additional 50 MCSs were similarly identified.

The environment during these periods was also examined for the condition of "widespread convection." This condition is defined as a highly concentrated group of thunderstorms that does *not* undergo upscale growth and organization into an MCS, meaning that the objective satellite-based definition of an MCS is not met. Two examples of widespread convection are shown in Figs. 6 and 7 to provide an idea of how this condition evolves in radar and satellite imagery. During the warm seasons of 1996–98, there were 300 instances of widespread convection identified, while 33 cases were documented during BAMEX. Please note that widespread convection can exist at the same time that an MCS is present somewhere else over the central United States. Several different methods, described below, were used to analyze the precursor environments of MCSs and widespread convection.

One type of data used in the analysis was surface analyses produced by the Hydrometeorological Prediction Center (HPC) of the National Centers for Environmental Prediction (NCEP). These surface analyses are subjectively analyzed by HPC forecasters every 3 h (i.e., 0000, 0300, 0600 UTC, etc.) for surface pressure, fronts, troughs, outflow boundaries, and drylines (see Fig. 8). These surface analyses were used as a starting point in the identification of any detectable initiating mechanism that generated the initial convection for each MCS during the dependent study period. Radar data were used to locate the original convective cells that underwent upscale growth into a mature MCS. The

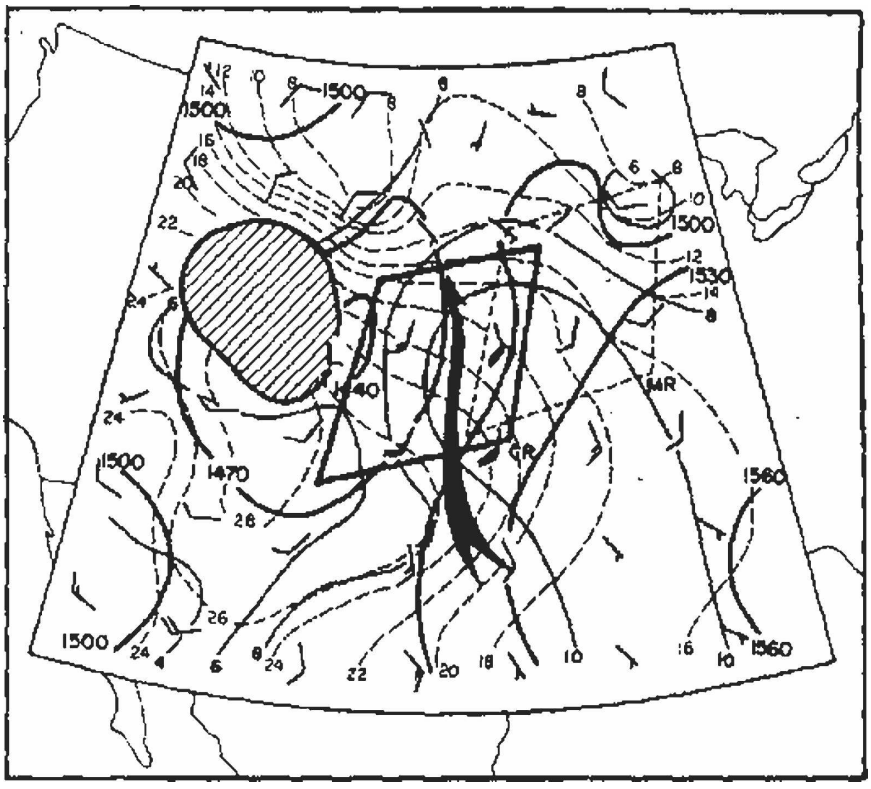

FIG. 2. Analysis of the 850-hPa level prior to MCC development. The thick solid lines are height contours (m), the dashed lines are isotherms (°C), and the thin solid lines are mixing ratios (g kg^{-1}). Full wind barbs represent 5 m s^{-1}, and a flag represents 25 m s^{-1}. The dark arrow indicates the axis of maximum winds. The genesis region is indicated by the solid quadrilateral. The hatched region indicates surface elevations above 850 hPa (from Maddox 1983).

surface observations were then examined, paying particular attention to the temperature gradient (see Sanders and Doswell 1995) and keeping the position and orientation of the convection in mind to locate and identify initiating features. If the convection began near a feature that likely influenced its development, then that feature was recorded to be associated with the initial convection of the MCS. In the same manner, the initiating mechanisms for the cases of widespread convection were identified for comparison with the MCS triggers. The results of this subjective analysis are presented in section 4a.

Data from the NCEP North American Regional Reanalysis (NARR) were also used to examine the precursor environments of MCSs (data missing for 4 of 387 MCSs) and widespread convection in this study. Reanalysis data are generated by a slightly modified version of the 2003 operational Eta Model and 3DVAR Data Assimilation System (EDAS) (Mesinger et al. 2006). These analyses are of relatively high resolution with 32-km horizontal grid spacing, 45 vertical layers, and 3-h intervals. The NARR improves upon the NCEP Global Reanalysis in resolution and accuracy owing to modeling and data assimilation improvements, as well as the incorporation of more data (e.g., precipitation, profiler winds, and surface winds and moisture) (Mesinger et al. 2006). The NARR provides a long-term, consistent, high-resolution dataset to examine the environment prior to the development of MCSs over the United States. During BAMEX, analyses and forecasts generated by the operational Eta Model and EDAS were used to examine the environmental conditions.

Numerous basic (e.g., height, wind, moisture, and temperature) and derived (e.g., divergence, vorticity, and advection) fields were examined from these datasets to identify features important to MCS development. One method used in this analysis involved simply taking a single value of a given field for each event at a specific point. For MCSs, the data were extracted at 6 h prior to development from the location of the −52°C cloud shield centroid of the MCS at initia-

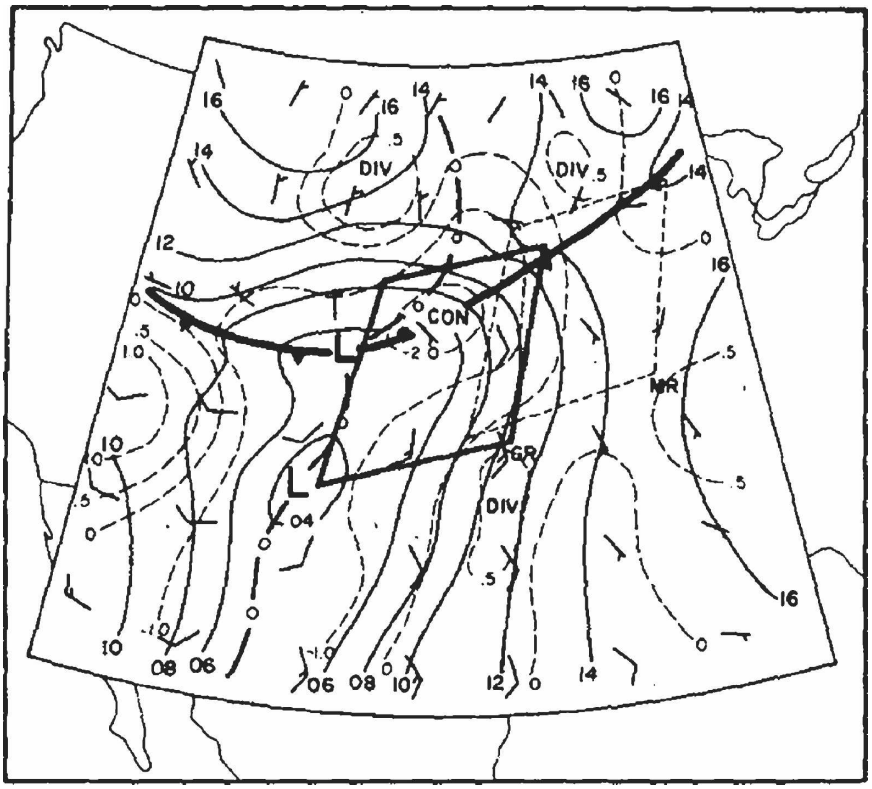

FIG. 3. Analysis of surface features prior to MCC development, including fronts and troughs. The solid lines represent mean sea level pressure, the dashed lines represent divergence (10^{-5} s^{-1}), and full wind barbs represent 5 m s^{-1} (from Maddox 1983).

tion. For widespread convection, data were taken from the approximate center of the group of thunderstorms at the time of the maximum number of convective cells. Once all of the point-value data were collected, typical parameter ranges and values were compared for the different conditions, allowing for a statistical analysis of the data discussed in section 4b.

Storm-relative composites were created for the precursor environment of MCSs and for the cases of widespread convection. A 20° × 15° movable grid centered on each storm was used to create composites of numerous parameters. For a given parameter, the deviation from the grid mean was averaged at each grid point over every storm to get a composite of the deviation values. The average of the grid means was then added to the composited deviation values to get meaningful meteorological quantities. This method of compositing the deviation values helps reduce the uncertainty that arises from parameters with seasonally varying means (Anderson and Arritt 1998). Finally, the data were filtered with a one-pass Barnes filter (Barnes 1964; Doswell 1977) using a response function similar to that of Anderson and Arritt (1998) to remove the small-scale noise that results from compositing. The composite maps were also checked against the distribution of parameter values to ensure that they resembled the majority of their ensemble members. For example, if more than three-fourths of the MCSs in the sample revealed a certain trait (e.g., 700-hPa warm air advection, 850-hPa southerly flow, etc.), then that feature was expected to be evident in the composite maps. The storm-relative composites, which allow for the retention of some of the mesoscale features important to MCS development (Maddox 1983; Cotton et al. 1989), are revealed in section 4c.

An objective method was also implemented to test the skill and accuracy of the various parameters in forecasting MCSs. This method involved making a dichotomous forecast, where a forecast was given (i.e., yes or no) based on a varying threshold value and whether or not an MCS was observed. From the resulting contingency table, numerous measurements of accuracy and skill [e.g., probability of detection (POD), false alarm ratio (FAR), bias (B), threat score (TS), and Heidke skill score (HSS); Wilks (1995)] can be calculated to evaluate objectively the value of different environmental parameters in forecasting MCSs. The results of this analysis are conveyed in section 4d.

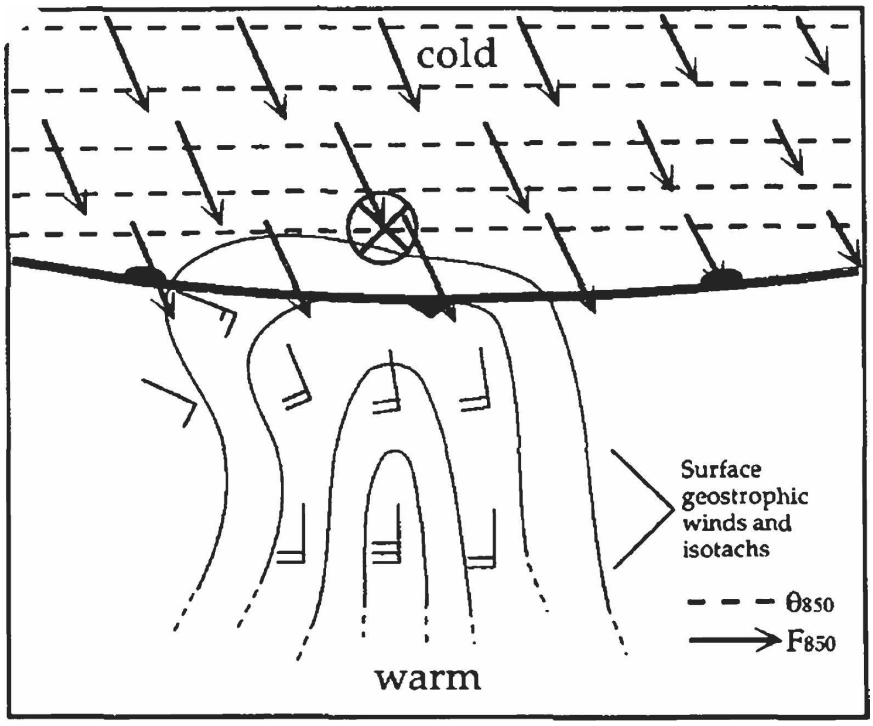

FIG. 4. Schematic of the probable location (circled times sign) of a large MCS at maturity. The thin solid lines represent the late-afternoon surface geostrophic isotachs where a full wind barb represents 5 m s^{-1}, the dashed lines represent the 850-hPa isentropes at 0000 UTC, and the arrows represent the 850-hPa frontogenesis vectors at 0000 UTC (from Augustine and Caracena 1994).

4. Analysis of environmental conditions

a. Initiating mechanisms

The distribution of the initiating mechanisms for MCSs and widespread convection is shown in Table 1. MCS convection was most frequently initiated by stationary fronts (27% of sample), cold fronts (21%), and troughs (18%). For the condition of widespread convection, troughs (27%), stationary fronts (15%), cold fronts (13%), and orographic influences (13%) were the most common initiating mechanisms. Additionally, one-third of the cases of widespread convection did not have an identifiable initiating mechanism. MCSs have been documented in previous studies to develop in the vicinity of fronts (Maddox 1983; McAnelly and Cotton 1986; Smull and Augustine 1993; Trier and Parsons 1993), so it is not surprising that stationary fronts and cold fronts were most commonly associated with MCS initiation. However, convection that develops along a frontal boundary is not guaranteed to develop into an MCS with more than one-fourth of the widespread convection cases being initiated along a frontal boundary. This suggests that strong low-level ascent (e.g., along a frontal boundary) and instability, which favor convective development, are often not sufficient conditions to support long-lived MCSs. Hence, there must be other features present in the ambient environment that aid MCS development.

Drylines are also common zones of thunderstorm formation (Rhea 1966); however, they apparently are not very favorable locations for MCS development as less than 5% of the MCSs in this sample developed along a dryline. In agreement with this result, Parker and Johnson (2000) found that the dryline was associated with only 8% of the MCSs they studied. Additionally, only 1% of the widespread convection cases in this study were initiated by drylines, indicating that thunderstorms do not often develop in high concentrations along a dryline. Thus, the overall isolated nature of the convection in the vicinity of the dryline limits the possibility of interaction among convective cells and upscale growth into an MCS.

b. Statistical analysis

A statistical analysis of point-value data was performed to compare the precursor environments of MCSs and widespread convection. The tables throughout this section list the average and standard deviation

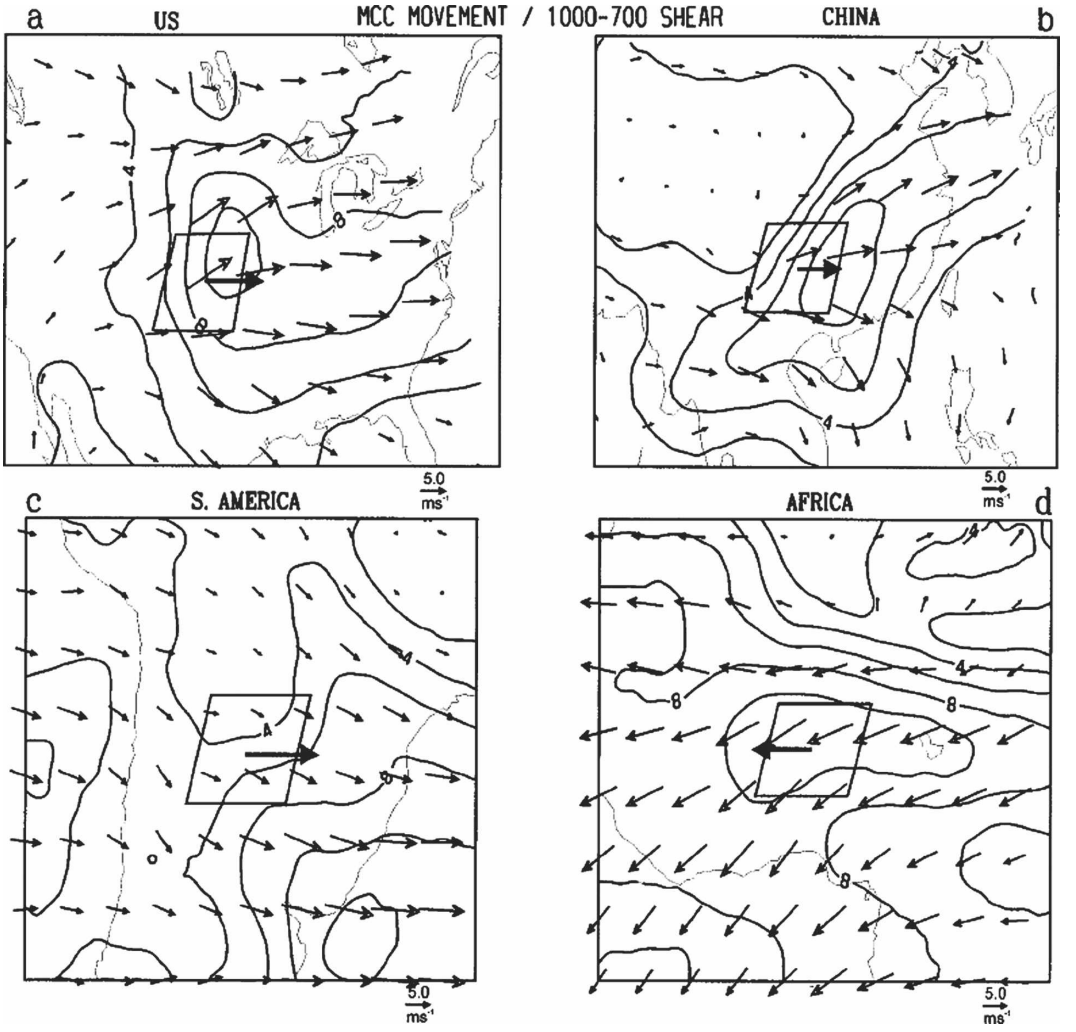

FIG. 5. The 1000–700-hPa vertical wind shear for MCC populations around the globe. The solid contours represent the magnitude of the shear ($m\ s^{-1}$). The shear vectors are the smaller arrows while the large, boldface arrows represent MCC motion. The quadrilaterals represent the MCC genesis regions (from Laing and Fritsch 2000).

of numerous parameters for these different conditions. A *t* test was performed to determine if the mean of the parameters in the MCS precursor environment differs from the widespread convection condition at the 99% confidence level. In addition, the first quartile, median, and third quartile values are listed for parameters that frequently take either positive or negative values (e.g., temperature advection).

Upper-level divergence and **Q**-vector convergence prior to MCS development are not statistically significantly different from the condition of widespread convection (see Table 2). In fact, only about half of the MCS precursor environments exhibit upper-level divergence and **Q**-vector convergence. Thus, it would be difficult to identify an MCS environment based on upper-level parameters alone. From the ω equation of quasi-geostrophic theory, one would expect a contribution to the upward vertical motion in a region of positive differential vorticity advection. However, positive vorticity advection at 500 hPa does not appear to be an important feature to the development of MCSs, which is in agreement with the findings of Maddox and Doswell (1982). In fact, the mean and median values of 500-hPa vorticity advection are actually negative for the precursor environment of MCSs, which typically would not favor storm development.

The values of midlevel potential vorticity (PV; i.e., 320 K) are not necessarily what one would expect for the different conditions. A positive PV anomaly usually develops in the middle troposphere owing to the heat-

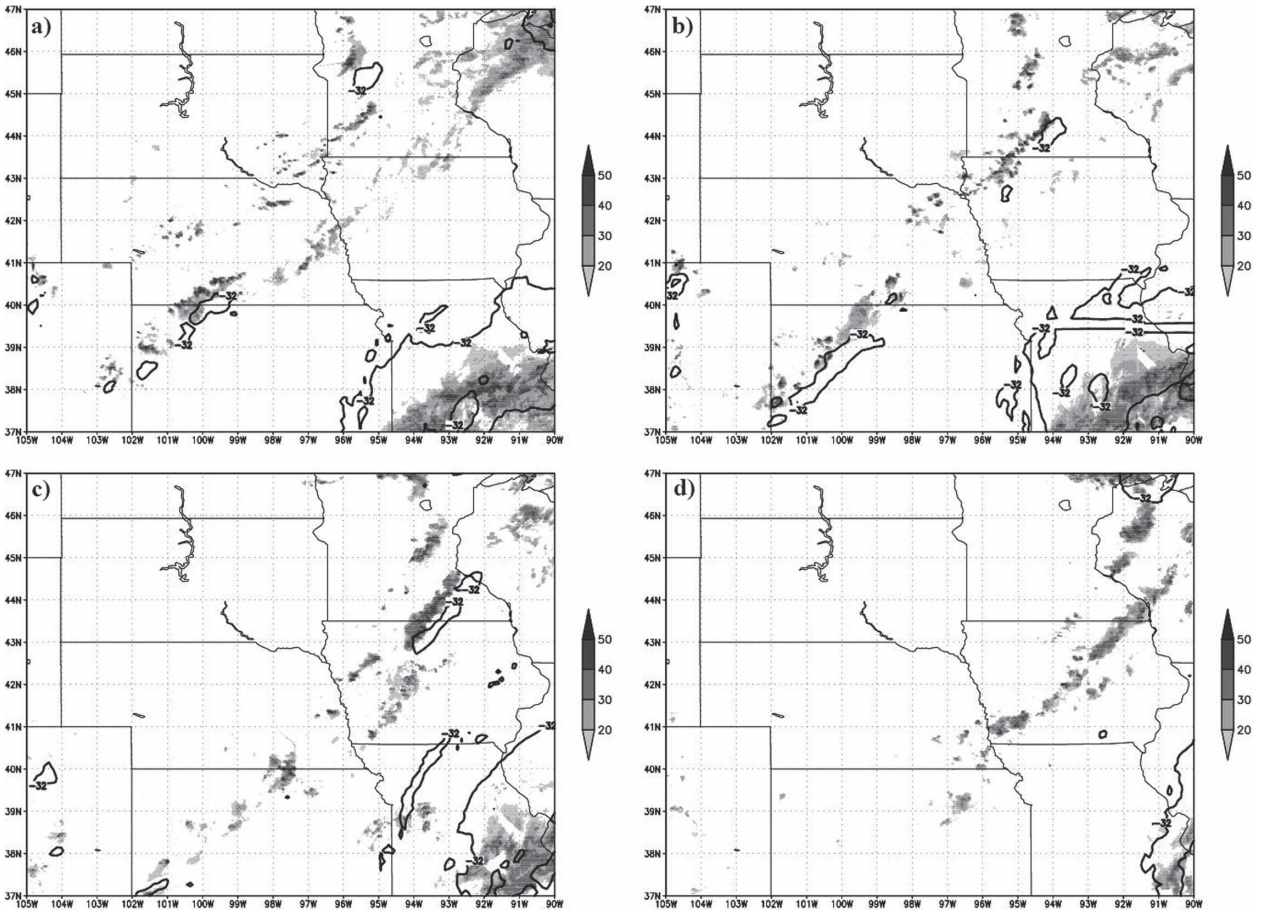

FIG. 6. Example of widespread convection that developed along a cold front from MN through KS, as seen by radar reflectivity (shaded) and IR satellite imagery (contoured at −32° and −52°C). The images are from (a) 2100 and (b) 2300 UTC 17 Jun and (c) 0100 and (d) 0400 UTC 18 Jun 1997.

ing profile within the stratiform region of MCSs (Hertenstein and Schubert 1991; Olsson and Cotton 1997). Several cases have been noted in which a midlevel, MCS-generated PV anomaly has led to ensuing convection and MCS development (e.g., Johnson et al. 1989; Fritsch et al. 1994). The results from this study reveal that widespread convection typically develops in a region of higher midlevel PV than MCSs. This finding does not dispel the notion that midlevel positive PV anomalies can enhance convective development and sustenance by the lifting of low-level air (Raymond and Jiang 1990). The result merely suggests that a positive PV anomaly is not a sufficient condition for the development of an MCS, meaning that other environmental features must be present in order to support the upscale growth of convective storms into an MCS.

Although the upper and middle levels reveal slight differences between the environments, the lower levels show more significant differences. The temperature advection at 700 hPa is much stronger (at >99% statistical significance) for the MCS precursor environment than for the widespread convection condition (see Table 3) with nearly an order of magnitude difference in the median. More than three-fourths of the MCSs have warm air advection at 6 h prior to initiation, signifying the importance and recurrent nature of this parameter to MCS development. Similar to differential vorticity advection, warm air advection also indicates rising motion according to the ω equation of quasigeostrophic theory. Thus, this existing, ambient upward vertical motion aids in the development and sustenance of MCSs (Maddox and Doswell 1982; Maddox 1983; Cotton et al. 1989; Laing and Fritsch 2000).

At 850 hPa, southerly component flow is present prior to the development of more than three-fourths of the MCSs in this study (Table 3). The winds at 850 hPa are routinely used as a proxy for the LLJ, which has often been noted as a recurrent feature of the MCS precursor environment (Maddox 1983; Cotton et al. 1989; Anderson and Arritt 1998; Laing and Fritsch

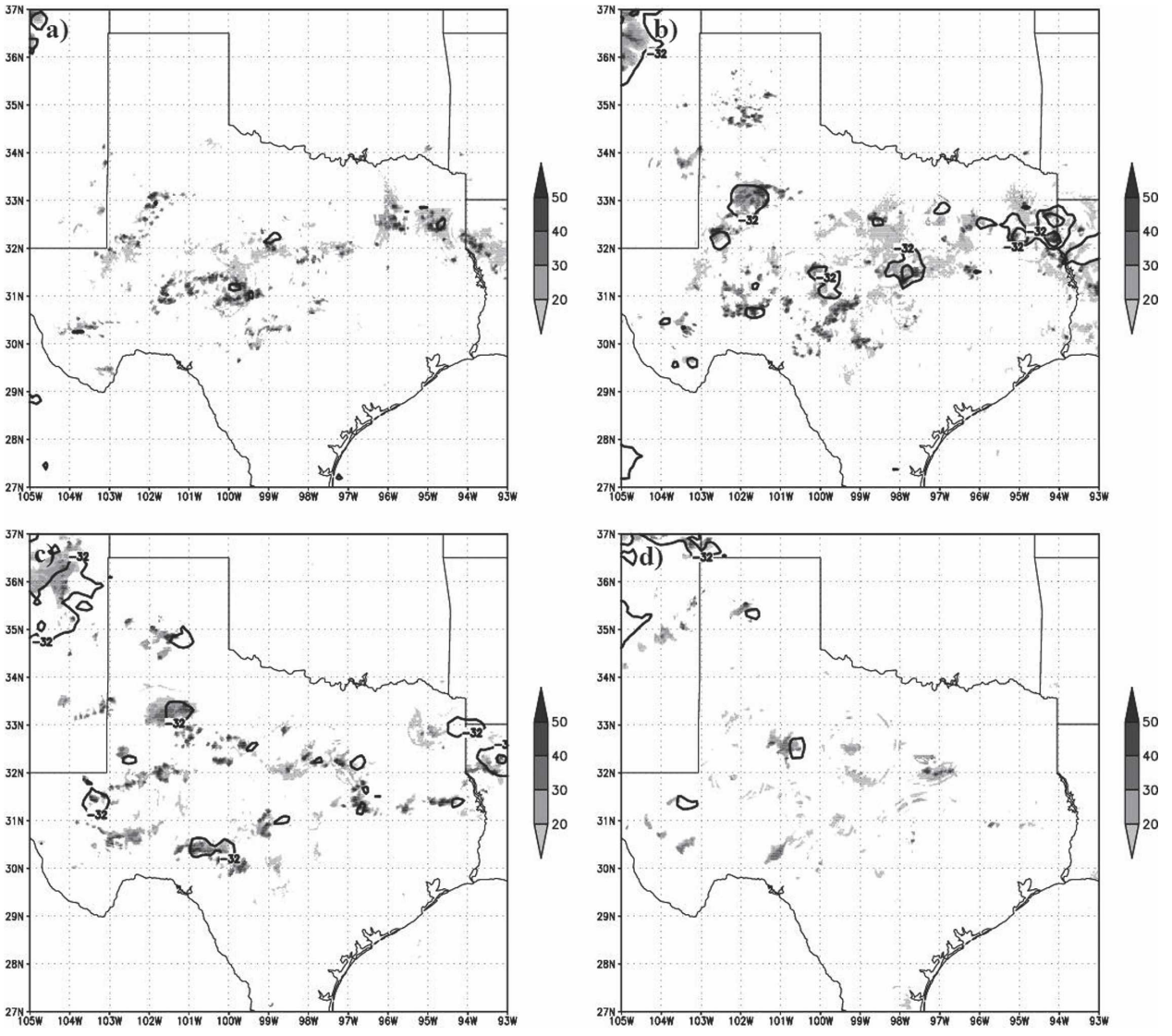

FIG. 7. Example of widespread convection across TX, as seen by radar reflectivity (shaded) and IR satellite imagery (contoured at −32° and −52°C). The images are from (a) 2000 and (b) 2200 UTC 16 Jul and (c) 0000 and (d) 0300 UTC 17 Jul 1998.

2000). Somewhat surprisingly, however, other features are not as prominent at 850 hPa. Convergence, warm air advection, and frontogenesis all existed for more than half of the MCS precursor environments, but the averages are not different from the condition of widespread convection at a statistical significance of 99%. At the surface (see Table 4), the MCS precursor environment is very moist with an average surface specific humidity of 13.5 g kg^{-1} (~18°C surface dewpoint temperature). Surface convergence is commonly found prior to MCS development, but the values are not statistically different from the average environment of widespread convection at the 99% confidence level.

The stability parameters [surface-based CAPE, best four-layer lifted index (LI), severe weather threat index (SWEAT)] in Table 5 indicate that MCSs typically develop in more unstable environments than does widespread convection. Interestingly, the CIN for the MCS precursor environment is much larger on average than for the condition of widespread convection. This result may suggest that a modest cap may be important for explosive, simultaneous convection resulting in the interaction of thunderstorms rather than weaker CIN, which could lead to sporadic thunderstorm generation, or larger CIN, which could prevent convective initiation all together.

The winds are stronger on average at the 99% statis-

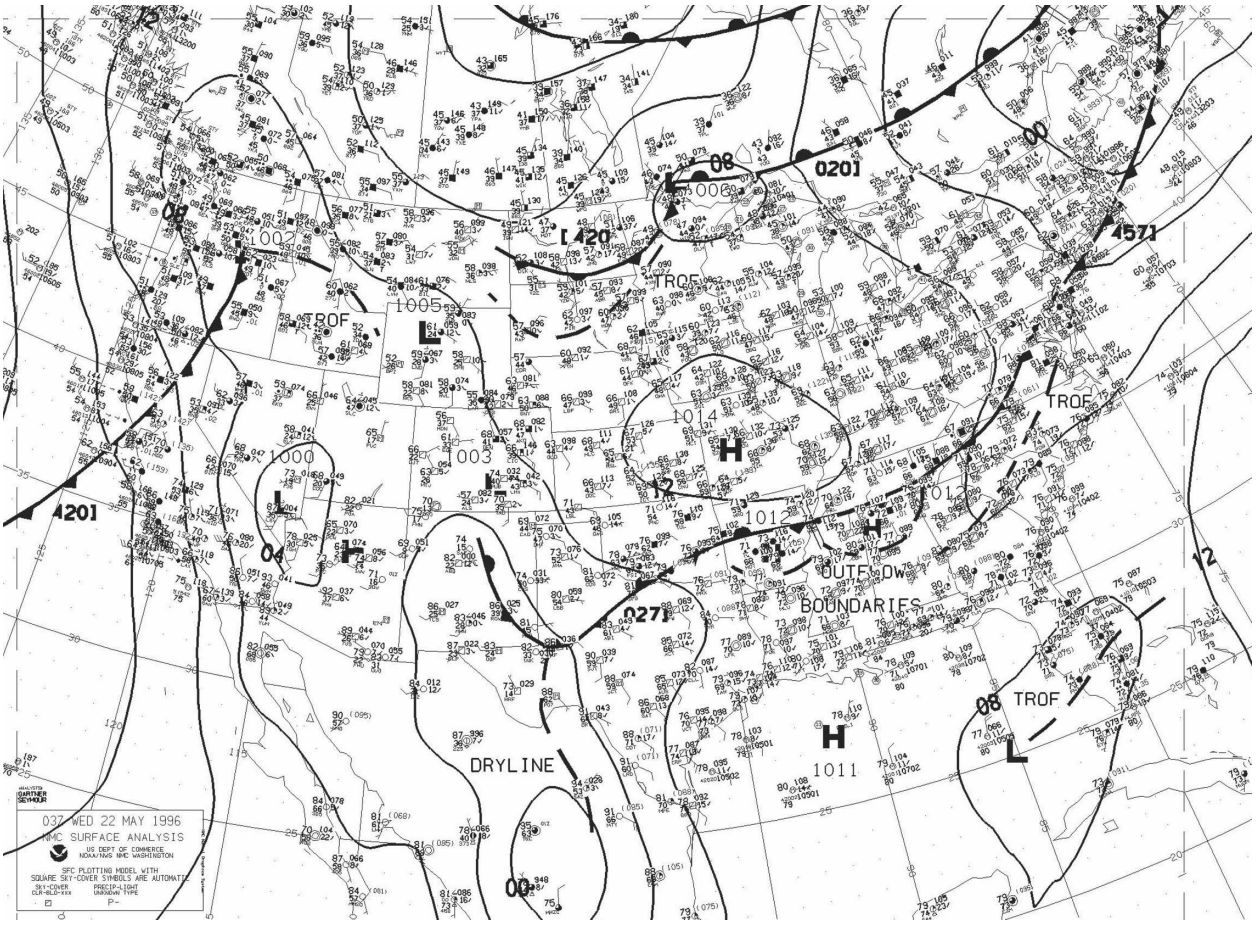

FIG. 8. NCEP surface analysis for 0300 UTC 22 May 1996. This example shows the analysis of fronts, troughs, outflow boundaries, and a dryline.

tical significance level for the MCS precursor environment than the environment of widespread convection through the entire depth of the troposphere down to the surface (see Table 6). The MCS precursor environment also has larger vertical wind shear than the environment of widespread convection through the lower half of the troposphere (see Table 7). The magnitude of shear over the lowest 1, 3, and 6 km of the atmosphere along with values of 0–3-km storm-relative helicity (SRH) are all statistically larger at the 99% significance level for environments that sustain organized convection. Thus, convection that undergoes an upscale-growth process commonly appears to be associated with large vertical wind shear.

c. *Storm-relative composites*

Note that the map background in the storm-relative composites simply provides a reference of the sizes of various features and the average initiation locations of the storms. The average centroid of initiation for MCSs in this sample was 38.38°N, 97.38°W at 0100 UTC (composites taken at 6 h prior = 1900 UTC), whereas the average location of widespread convection was 37.32°N, 96.57°W at 2130 UTC. In the upper and middle levels (composites not shown), the environments that support convective organization and those that do not support convective organization appear qualitatively similar. At 300 hPa, an area of modest divergence exists prior to the development of MCSs and widespread convection, but MCSs typically develop just upstream of an upper-level ridge while widespread convection generally forms downstream of a ridge in a region of much weaker winds. At 500 hPa, a more favorable pattern of positive vorticity advection exists for widespread convection than for MCSs.

Warm air advection at 700 hPa appears to be a particularly good indicator of MCS development, as the maximum coincides with the future location of MCS

TABLE 1. Distribution of initiating mechanisms for MCSs and widespread convection.

Initiating mechanism	MCS	Widespread convection
Stationary front	104	45
Cold front	81	40
Warm front	26	6
Trough	69	80
Orographic influence	48	39
Dryline	16	4
Outflow boundary	9	4
Multiple features (included in totals above)	39	19
Orographic influence and trough	17	14
Orographic influence and stationary front	11	3
Orographic influence and cold front	2	1
Orographic influence and dryline	1	0
Trough and stationary front	2	1
Trough and cold front	2	0
Trough and warm front	1	0
Stationary front and cold front	1	0
Stationary front and dryline	1	0
Stationary front and outflow boundary	1	0
Other (e.g., triple point and MCV)	8	2
Unidentified	65	99
Tot	387	300

TABLE 2. Point-value data of upper- and midlevel parameters for the MCS precursor environment and widespread convection. For each parameter, the mean and standard deviation (σ) are listed, where boldface numbers indicate that the mean MCS precursor environment is different from the widespread convection environment at the 99% confidence level. For some parameters, the first-quartile (1Q), median, and third-quartile (3Q) values are also listed.

Parameter		MCS −6 h	Widespread convection
300-hPa divergence (s^{-1})	Mean	3.4×10^{-6}	2.7×10^{-6}
	σ	1.9×10^{-5}	1.6×10^{-5}
	1Q	-7.0×10^{-6}	-5.6×10^{-6}
	Median	1.6×10^{-6}	2.4×10^{-6}
	3Q	1.0×10^{-5}	1.1×10^{-5}
300 **Q**-vector divergence ($K\ m^{-2}\ s^{-1}$)	Mean	7.2×10^{-16}	-5.1×10^{-16}
	σ	1.1×10^{-14}	7.5×10^{-15}
	1Q	-1.8×10^{-15}	-1.7×10^{-15}
	Median	-4.7×10^{-17}	2.0×10^{-16}
	3Q	2.2×10^{-15}	2.0×10^{-15}
500-hPa vorticity advection (s^{-2})	Mean	-3.1×10^{-10}	4.7×10^{-10}
	σ	4.9×10^{-9}	3.7×10^{-9}
	1Q	-1.9×10^{-9}	-6.3×10^{-10}
	Median	-9.4×10^{-11}	1.8×10^{-10}
	3Q	1.6×10^{-9}	1.2×10^{-9}
320-K potential vorticity (PVU)	Mean	**0.42**	**0.81**
	σ	0.41	1.01

initiation while the magnitude is much less for widespread convection (cf. Figs. 9a and 9b). In addition, the warm air advection pattern indicates a sharp decrease to the west, but a broad area of high values that extends to the east, which suggests that eastward-moving MCSs will remain in an environment favorable for survival. At 850 hPa, a well-defined short-wave trough and its associated convergence are clearly evident prior to MCS development to the west of the point of MCS initiation (see Figs. 9c and 9d). Likewise, a maximum of convergence is coincident with the center of the widespread convection composite; thus, low-level convergence is also important for the convective initiation of thunderstorms that do not organize into an MCS. The biggest difference at this level between the environments can be seen in the wind field. In the MCS composite, the LLJ feeds into the MCS initiation location whereas the composite of widespread convection reveals no distinct LLJ with much weaker winds throughout the region. Composite surface features (not shown) are similar to those at 850 hPa, including the convergence and wind fields.

The stability parameters in Figs. 9e and 9f show a region of unstable stratification that extends from the southeast toward the center of each composite. The LI seems to locate convective development better than CAPE, as indicated by the minimum LI value (i.e., most unstable region) reaching more closely to the center of the composites. Overall, the MCS precursor environment is more unstable than the environment of widespread convection with larger CIN. The low-level vertical wind shear is much greater in the MCS precursor environment than in the widespread convection environment. The magnitudes of the 0–3-km shear vector and SRH have a maximum value very near the location of MCS initiation (see Figs. 9g and 9h). The widespread convection composite also reveals a maximum in low-level shear near the center, but the magnitude and gradient are much less than in the MCS composite.

d. Dichotomous forecasting

A dichotomous forecasting method was employed to evaluate parameters objectively in their ability to forecast MCSs. Rasmussen and Blanchard (1998) utilized this method to discriminate among the environments of supercell thunderstorms with significant tornadoes, supercells without significant tornadoes, and ordinary thunderstorms. A similar approach was used here to discriminate between MCS precursor environments and widespread convection environments. Numerous forecast accuracy and skill measures (i.e., HSS, TS, POD, FAR, and *B*) were calculated over a range of values for each parameter based on the 2×2 contin-

TABLE 3. Same as in Table 2 but for 700- and 850-hPa parameters.

Parameter		MCS −6 h	Widespread convection
700-hPa temp advection (K s^{-1})	Mean	**4.5×10^{-5}**	**6.8×10^{-6}**
	σ	7.3×10^{-5}	5.5×10^{-5}
	1Q	4.0×10^{-6}	-9.4×10^{-6}
	Median	3.3×10^{-5}	3.9×10^{-6}
	3Q	7.0×10^{-5}	2.2×10^{-5}
850-hPa v-component wind speed (m s^{-1})	Mean	**4.1**	**1.9**
	σ	4.7	4.4
	1Q	1.0	−0.4
	Median	3.7	2.0
	3Q	6.9	4.3
850-hPa moisture divergence (s^{-1})	Mean	-7.0×10^{-8}	-6.4×10^{-8}
	σ	2.7×10^{-7}	1.6×10^{-7}
	1Q	-2.0×10^{-7}	-1.3×10^{-7}
	Median	-4.9×10^{-8}	-4.5×10^{-8}
	3Q	7.6×10^{-8}	3.2×10^{-8}
850-hPa temp advection (K s^{-1})	Mean	3.1×10^{-5}	1.1×10^{-5}
	σ	8.9×10^{-5}	6.7×10^{-5}
	1Q	-7.0×10^{-6}	-1.2×10^{-5}
	Median	2.4×10^{-5}	3.4×10^{-6}
	3Q	6.4×10^{-5}	2.7×10^{-5}
850-hPa frontogenesis (s^{-1})	Mean	1.9×10^{-15}	3.1×10^{-15}
	σ	2.7×10^{-14}	2.7×10^{-14}
	1Q	-1.2×10^{-15}	-1.0×10^{-15}
	Median	3.3×10^{-16}	1.2×10^{-16}
	3Q	5.0×10^{-15}	1.9×10^{-15}

gency tables. HSS was considered to be the most appropriate measure of forecast skill because it gives credit to correct forecasts of nonevents, but also takes the false alarm ratio into account (Doswell et al. 1990). Therefore, the parameters with the highest HSSs were assumed to show the best capability of distinguishing the MCS precursor environments from widespread convection.

The parameters with the 10 highest HSSs for distinguishing between MCS precursor environments and environments of widespread convection (Table 8) generally perform as well as or better than the parameters

TABLE 4. Same as in Table 2 but for surface parameters.

Parameter		MCS −6 h	Widespread convection
Surface specific humidity (g kg^{-1})	Mean	**13.5**	**12.0**
	σ	3.7	4.1
Surface moisture divergence (s^{-1})	Mean	-7.6×10^{-8}	-6.8×10^{-8}
	σ	2.9×10^{-7}	2.1×10^{-7}
	1Q	-2.2×10^{-7}	-1.6×10^{-7}
	Median	-5.7×10^{-8}	-5.4×10^{-8}
	3Q	1.0×10^{-7}	3.2×10^{-8}

TABLE 5. Same as in Table 2 but for stability parameters.

Parameter		MCS −6 h	Widespread convection
CAPE (J kg^{-1})	Mean	**1560**	**1083**
	σ	1088	784
	1Q	695	464
	Median	1563	989
	3Q	2358	1594
LI (K)	Mean	**−4.4**	**−3.1**
	σ	3.3	2.4
	1Q	−6.6	−4.6
	Median	−4.9	−3.3
	3Q	−2.9	−1.8
SWEAT index	Mean	**307**	**238**
	σ	110	87
	1Q	222	184
	Median	304	220
	3Q	379	278
CIN (J kg^{-1})	Mean	**−53.2**	**−20.5**
	σ	67.4	45.9
	1Q	−74.0	−16.6
	Median	−28.8	−3.4
	3Q	−7.0	−1.0

used in the studies of Rasmussen and Blanchard (1998) and Rasmussen (2003) for supercell and tornado forecast parameters. The FAR is notably lower in this study as opposed to the tornado-related studies. SRH had the highest HSS in this study at an optimal value of 60 m^2 s^{-2}, meaning that MCSs would be expected to develop from a highly concentrated group of thunderstorms only for values of SRH larger than this threshold. Shear parameters tend to be the best at distinguishing between MCS environments and environments that do not support organized convection. Five out of the top 10 parameters are based on or incorporate vertical wind shear, including the SWEAT index, which is

TABLE 6. Same as in Table 2 but for wind speed.

Parameter		MCS −6 h	Widespread convection
300-hPa wind speed (m s^{-1})	Mean	**19.9**	**16.4**
	σ	10.4	11.8
500-hPa wind speed (m s^{-1})	Mean	**14.5**	**10.3**
	σ	6.4	6.8
700-hPa wind speed (m s^{-1})	Mean	**9.4**	**7.2**
	σ	4.9	4.7
850-hPa wind speed (m s^{-1})	Mean	**7.4**	**5.7**
	σ	4.3	4.0
Surface wind speed (m s^{-1})	Mean	**4.4**	**3.8**
	σ	2.1	1.9

TABLE 7. Same as in Table 2 but for shear parameters.

Parameter		MCS −6 h	Widespread convection
0–1-km shear ($m\ s^{-1}$)	Mean	**5.1**	**3.1**
	σ	3.7	3.2
	1Q	2.4	1.1
	Median	4.3	2.0
	3Q	6.7	3.8
0–3-km shear ($m\ s^{-1}$)	Mean	**11.5**	**7.7**
	σ	5.0	4.9
	1Q	7.9	4.0
	Median	11.0	6.5
	3Q	14.8	10.4
0–6-km shear ($m\ s^{-1}$)	Mean	**16.5**	**11.3**
	σ	7.3	8.0
	1Q	11.1	5.6
	Median	16.3	9.4
	3Q	21.5	15.4
Storm-relative helicity ($m^2\ s^{-2}$)	Mean	**126.8**	**69.8**
	σ	93.5	79.3
	1Q	66.2	23.1
	Median	106.0	45.8
	3Q	168.2	94.8

heavily weighted by wind shear. Three stability parameters (CAPE, CIN, and LI) and 700-hPa temperature advection are also among the best MCS forecast parameters.

5. MCS index

The previous section provided significant insight into environmental features that help determine whether convection will evolve into an MCS. These results may be even more useful to forecasters if they could be *directly* applied to MCS forecasting through an index. Like other weather indices, an MCS index is an objective tool to help forecasters make difficult decisions about the possible development of MCSs. Given the difficulty of forecasting convective initiation, an MCS index would not be expected to forecast every MCS accurately and may overpredict MCSs in some situations. The MCS index introduced here simply indicates areas that are favorable for MCS development and sustenance given that a highly concentrated group of thunderstorms has formed.

The analysis of environmental conditions discussed earlier focused on the conditions 6 h prior to MCS initiation. Consequently, the MCS index defined here implicitly provides a forecast out to 6 h of conditions favorable for MCSs. The parameters selected to be in the MCS index were chosen based on the analysis of the MCS precursor environment versus the environment of widespread convection, as presented in section 4. Consequently, the value of the index reflects the likelihood that thunderstorms will develop into an MCS. The MCS index is defined below:

$$\text{MCS Index} = \frac{-(\text{LI} + 4.4)}{3.3} + \frac{(\text{0–3-km shear} - 11.5\ \text{m s}^{-1})}{5\ \text{m s}^{-1}} + \frac{(\text{700-hPa TA} - 4.5 \times 10^{-5}\ \text{K s}^{-1})}{7.3 \times 10^{-5}\ \text{K s}^{-1}}.$$

The MCS index is composed of three terms: LI, 0–3-km shear, and 700-hPa temperature advection (TA), where the MCS sample mean of each parameter is subtracted from its value at a given location and divided by the sample standard deviation, so the terms could be combined into a unitless index. Different forms of the index were evaluated along with different methods (e.g., classification and regression trees) in forecasting MCSs, but the functional form of the index proved to be as accurate (i.e., in terms of a maximum HSS) as any form with the advantage of being simple and straightforward. It is worth noting that the MCS index should only be examined where convective development is probable (e.g., LI < 0 or CAPE > 0). The following discussion expands on the rationale used in choosing the parameters included in the MCS index.

A stability parameter is a necessary component of the MCS index to identify environments that are capable of generating and supporting deep convection. The LI was chosen over CAPE because it has a slightly higher HSS in distinguishing MCS environments from unorganized widespread convection (see Table 8) and better encompasses the location of MCS initiation (see Fig. 9e). In addition, the LI indicates the most unstable of four layers within 180 hPa of the surface using a continuous range of values.

Warm air advection at 700 hPa has been documented as a recurrent feature of the MCS precursor environment. As mentioned previously, it signals an area of ambient rising motion, which is beneficial for thunderstorm generation and organization. The results from this study show that MCSs develop in areas of significantly stronger warm air advection at 700 hPa than thunderstorms that do not evolve into MCSs (see Table 8). In addition, the maximum in the composite 700-hPa temperature advection field is perfectly collocated with the average location of MCS initiation (see Fig. 9a). Even though warm air advection is also often found at 850 hPa prior to MCS development, more systems tend to develop in warm air advection at 700 hPa; thus, the 700-hPa level was chosen to diagnose temperature advection.

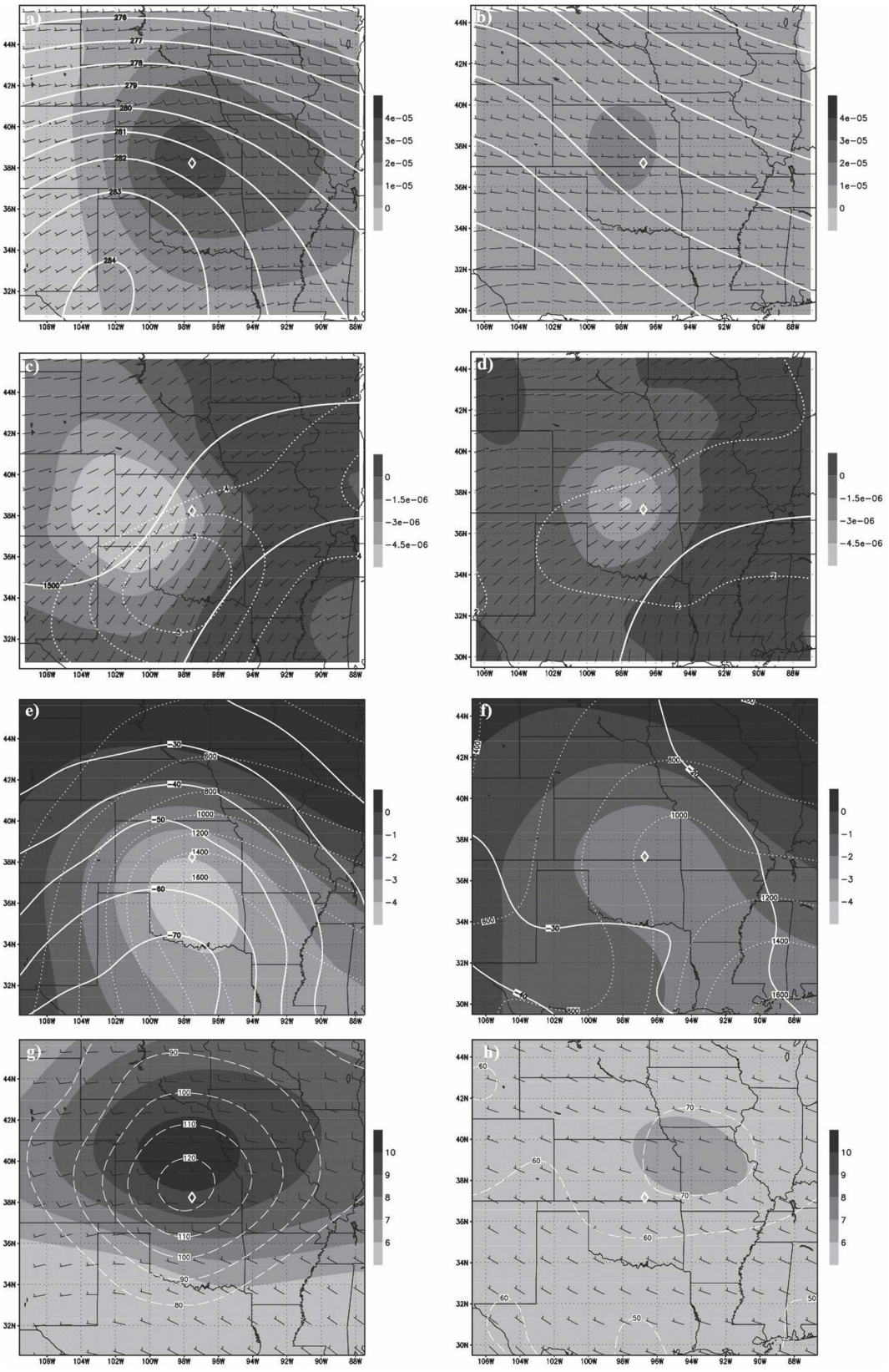
a)
276
277
278
279
280
281
282
283
284
4e−05
3e−05
2e−05
1e−05
0
b)
4e−05
3e−05
2e−05
1e−05
0
c)
0
−1.5e−06
−3e−06
−4.5e−06
1500
d)
0
−1.5e−06
−3e−06
−4.5e−06
e)
−30
−40
−50
−60
−70
800
900
1000
1200
1400
1600
0
−1
−2
−3
−4
f)
1400
800
1000
1200
1400
1600
0
−1
−2
−3
−4
g)
90
100
110
120
110
100
90
80
10
9
8
7
6
h)
60
70
60
70
60
60
50
50
10
9
8
7
6

Examination of Table 8 reveals that lower-tropospheric shear over many depths is very good at determining whether convection will organize into an MCS. Prior studies of the precursor environments of MCSs have not emphasized low-level shear, but this study strongly suggests that low-level shear should be included in the MCS index. The 0–3-km shear was selected for the MCS index owing to its slightly higher HSS than either the 0–1- or 0–6-km shear. Additionally, the diurnal behavior of the 0–3-km shear more closely resembles the diurnal behavior of MCSs (i.e., nighttime maximum) than the 0–6-km shear owing to its more intimate relationship with the nocturnal LLJ (cf. Figs. 10 and 11). SRH was not chosen for the index because it includes a combination of two factors: the magnitude of the ambient shear vector, which enhances lifting at the leading edge of the cold pool, and veering winds with height, which suggest warm air advection through this layer for the geostrophic component of flow. To separate these effects and simplify their interpretation, individual terms for temperature advection and shear were included in the MCS index.

Each of the three parameters in the MCS index represents a different physical mechanism that acts to enhance the vertical lifting by which convective development and organization can occur. Conceptually, low-level warm air advection supports storm initiation and development over a relatively large area by helping to lift the air to the level of free convection where the existing convective instability can be accessed. After the storms become well established, the ambient vertical wind shear further enhances upward motion at the leading edge of the storm-generated cold pools, which promotes storm interaction and organization. The combination of these mechanisms appears to be the most favorable setting that leads to MCS development.

6. Evaluation of the MCS index

Even though the MCS index was carefully formulated based on results from the observational analysis of hundreds of MCSs, it would be useful to demonstrate the effectiveness of the index by assessing its forecasting performance and other important attributes. The MCS index was evaluated for two different periods: the dependent study period (April–August 1996–98) from which the index was derived and an independent convective period during BAMEX (20 May–6 July 2003). The forecast accuracy of the MCS index was examined using the dichotomous forecasting technique while the diurnal, seasonal, and episodic behaviors of the index were inspected by means of composites and examples.

The dichotomous forecasting technique reveals that the MCS index performs better than any of the individual parameters examined previously in distinguishing between MCS precursor environments and environments of unorganized widespread convection (cf. first row of Tables 8 and 9). Additionally, the MCS index exhibits more accuracy during BAMEX than during the dependent study period, providing assurance that the MCS index is not an artifact of a particular convective season. As expected, the overall accuracy of the MCS index decreases as the forecast lead time increases, but even 60-h forecasts show considerable accuracy in distinguishing between MCS precursor environments and widespread convection. Based on these results, general guidelines for the likelihood of MCS development are introduced in Table 10, where low values of the index (i.e., <-1.5) represent unfavorable conditions for MCS development while positive values indicate more favorable conditions for MCSs.

a. Diurnal and seasonal cycles

MCSs typically form in the late afternoon and evening hours, reach a maximum size during the night, and dissipate in the morning hours (Maddox 1980; Jirak et al. 2003). The nocturnal tendency of MCSs must also be present in an index that attempts to predict these systems. The diurnal cycle of the MCS index was examined by creating fixed-point composites at 3-h intervals during the dependent study period. Figure 12 shows the diurnal cycle of the MCS index starting when the index is at a minimum at 1200 UTC (i.e., early morning). The magnitude of the MCS index increases steadily throughout the day to the east of the Rocky Mountains until it reaches a maximum over the high plains at 0300 UTC (i.e., late evening) and then decreases into the morning hours. Thus, the diurnal cycle

←

FIG. 9. Storm-relative composites for (left) 6 h prior to MCS development and (right) widespread convection. (a), (b) At 700 hPa, the solid lines are isotherms (K), and the shading represents temperature advection (K s^{-1}). (c), (d) At 850 hPa, the solid lines represent height contours (m), the dashed lines represent isotachs (m s^{-1}), and the shading represents divergence (s^{-1}). (e), (f) For the stability parameters, the solid lines represent CIN (J kg^{-1}), the dotted lines represent CAPE (J kg^{-1}), and the shading represents LI (K). (g), (h) For the shear parameters, the dashed lines represent SRH (m^2 s^{-2}) and the shading represents 0–3-km shear (m s^{-1}). Each full wind barb represents 10 m s^{-1}, and the white diamonds identify the average location of storm initiation.

TABLE 8. Parameters with the highest HSSs for distinguishing between MCS precursor environments and environments of widespread convection. The optimal value at the maximum HSS for each parameter is listed, as well as the TS, POD, FAR, and *B* calculated at that optimal value.

	HSS	Optimal value	TS	POD	FAR	*B*
SRH	0.42	60 $m^2 s^{-2}$	0.61	0.78	0.27	1.07
0–3-km shear	0.36	8 $m s^{-1}$	0.57	0.74	0.29	1.04
CIN*	0.36	−10 $J kg^{-1}$	0.55	0.69	0.27	0.95
0–6-km shear	0.35	12 $m s^{-1}$	0.55	0.70	0.29	0.99
700-hPa temperature advection	0.33	2×10^{-5} K s^{-1}	0.50	0.61	0.26	0.81
SWEAT index	0.33	275	0.49	0.59	0.25	0.79
0–1-km shear	0.32	3 $m s^{-1}$	0.52	0.67	0.29	0.93
LI*	0.27	−4 K	0.49	0.62	0.30	0.88
200-hPa temperature*	0.26	219 K	0.46	0.58	0.30	0.82
CAPE	0.24	1400 $J kg^{-1}$	0.44	0.55	0.30	0.79

* A "yes" forecast is given for values less than the optimal value.

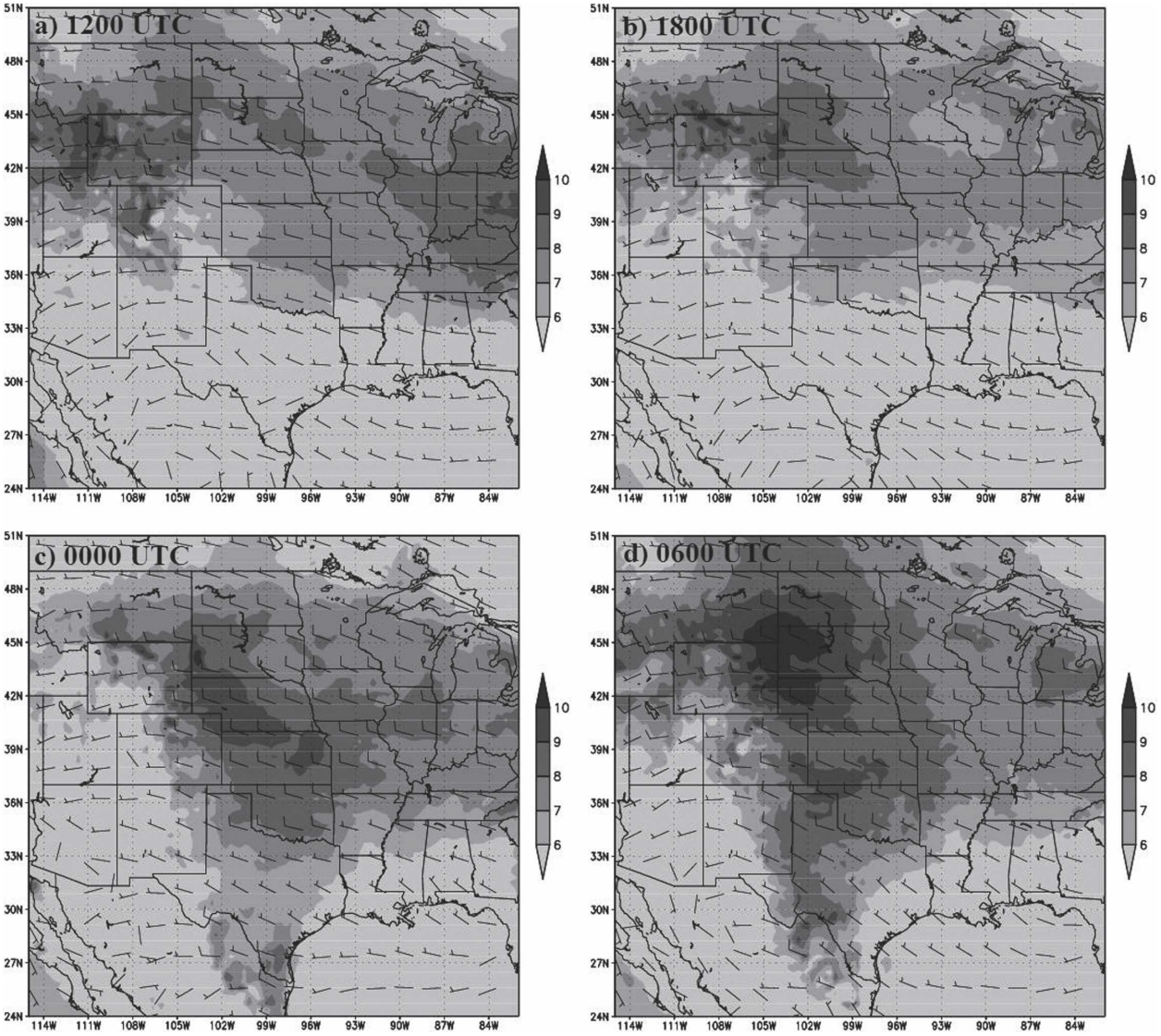

FIG. 10. Diurnal cycle of 0–3-km shear (shaded) as shown by fixed-point composites during the initial study period at 6-h intervals throughout the day. The shear vectors are displayed with a full barb representing 10 $m s^{-1}$.

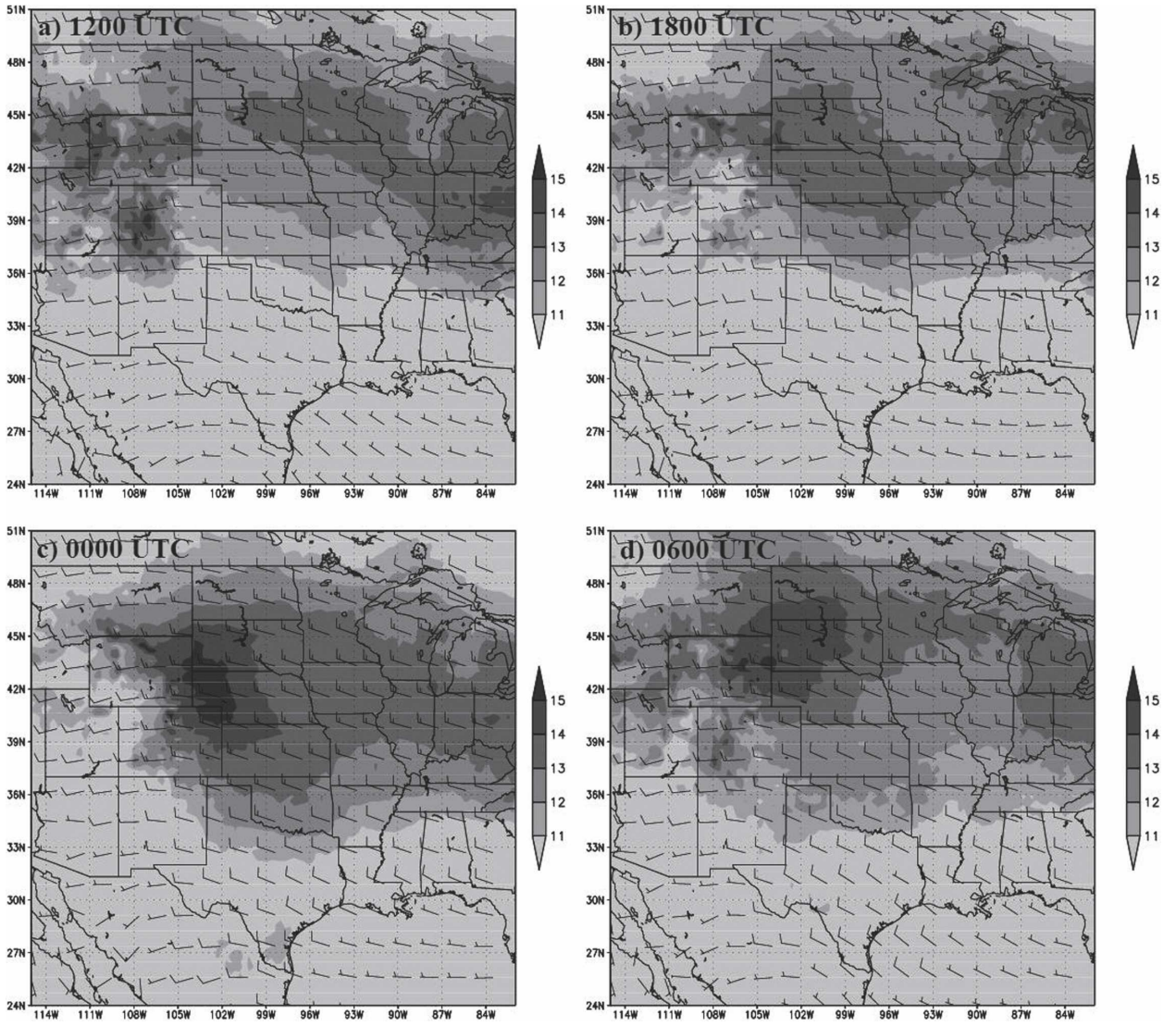

FIG. 11. Same as in Fig. 10 but for 0–6-km shear.

of the MCS index closely resembles the typical diurnal cycle of MCSs and properly indicates the nighttime as the most favorable period of MCS development and sustenance.

MCSs also have a distinct seasonal cycle, with the majority of systems forming during May–July over the central United States, shifting northward during the convective season (Fig. 13). The seasonal cycle of the

TABLE 9. Accuracy and skill measures of the MCS index in distinguishing between MCS precursor environments and widespread convection for reanalyses, analyses, and forecasts out to 60 h. The optimal value at the maximum HSS is listed, as well as the TS, POD, FAR, and *B* results calculated at that optimal value.

	HSS	Optimal value	TS	POD	FAR	*B*
Reanalysis (1996–98)	0.49	−1.5	0.66	0.85	0.25	1.14
Eta analysis (BAMEX)	0.54	−1.0	0.66	0.74	0.14	0.86
Eta 6–12-h forecast (BAMEX)	0.59	−1.5	0.69	0.74	0.10	0.82
Eta 18–24-h forecast (BAMEX)	0.51	−1.5	0.65	0.74	0.16	0.88
Eta 30–36-h forecast (BAMEX)	0.41	−1.5	0.55	0.62	0.16	0.74
Eta 42–48-h forecast (BAMEX)	0.41	−2.0	0.63	0.80	0.25	1.06
Eta 54–60-h forecast (BAMEX)	0.43	−1.5	0.57	0.64	0.16	0.76

TABLE 10. Guidelines for the likelihood of MCS development based on values of the MCS index given that a highly concentrated group of thunderstorms are present.

MCS index < -1.5 or undefined	Unfavorable
$-1.5 <$ MCS index < 0	Marginal
$0 <$ MCS index < 3	Favorable
MCS index > 3	Very favorable

MCS index was examined by creating fixed-point composites for each month during the 3-yr study period at the time of the maximum value of the index (i.e., 0300 UTC). Figure 14 reveals that the MCS index is at a minimum over the plains during April with conditions becoming much more favorable for MCSs during May–July. The maximum values of the MCS index also shift northward during the convective season in agreement with the observed northward shift of MCSs during the summer (cf. Figs. 13 and 14). The MCS index also coincides with another seasonal feature, increasing in magnitude and extent through July and August over northwestern Mexico and the southwest United States, which is consistent with the typical North American monsoon cycle (Douglas et al. 1993). The MCS index indicates that this region becomes more favorable for supporting organized, long-lived convection during the monsoon, leading to the seasonal precipitation maximum over northwestern Mexico and the southwestern United States.

b. Warm season precipitation episodes

Warm season precipitation episodes have been documented (Cotton et al. 1983; Carbone et al. 2002) as coherent sequences of MCSs that traverse the United States for periods of more than 1 day. Carbone et al. (2002) focused on precipitation events that occur under weakly forced midsummer conditions, owing to the relatively low skill in predicting convective precipitation by numerical weather models during this regime (Olson et al. 1995; Fritsch et al. 1998). To investigate the ability of the MCS index to forecast these episodes, the index is compared to radar-derived rain-rate Hovmöller diagrams from the Carbone et al. (2002) study. Several precipitation episodes can be seen in the right-hand panel of Fig. 15 as repetitive, coherent eastward-propagating features that typically begin east of the Continental Divide (~105°W) and cover around 1500 km over a 20–40-h period. Comparison of the MCS index to specific midsummer precipitation episodes reveals good correspondence with the timing and propagation of MCSs. Two different precipitation episodes are highlighted in Fig. 15 that demonstrate the association of coherent precipitation events and the MCS index. For example, the precipitation episode that started around 0000 UTC 20 July 1998 east of the Rocky Mountains and propagated eastward to the Appalachians by 1200 UTC 21 July 1998 is associated with a relative maximum in the MCS index.

Many other precipitation episodes and features in this figure are also consistent with the attributes of the MCS index. The index shows a definite diurnal cycle, with a maximum typically occurring shortly after 0000 UTC just east of the Continental Divide. That maximum progresses eastward overnight across the plains in response to the larger shear and advection due to the development of the LLJ. Finally, large values of the index are occasionally found on the following day near the Appalachians in response to decreased daytime stability. This results in a sort of "tiered" structure of the MCS index in the Hovmöller diagrams that encompasses the more smoothly propagating precipitation episodes. Even though the MCS index does not match up perfectly with all of the precipitation episodes (due in part to the convective initiation/regeneration issue), it still provides a good indication of the possible development of a midsummer precipitation episode. This result implies that convective instability, low-level shear, and low-level warm air advection are important to the existence of coherent, propagating precipitation systems.

c. Examples

A couple of representative examples were selected to demonstrate the usefulness and effectiveness of the MCS index in forecasting MCSs for a variety of situations. The first example is of an MCS that formed over eastern Nebraska and Kansas on 12 May 1998 (Fig. 16). By 0000 UTC, a line of thunderstorms forms along a cold front on the western boundary of the region favorable (i.e., MCS index > 0) for MCS development. As this convection advances eastward, it enters an area primarily favorable for MCS development and organizes into a narrow, leading-line–trailing-stratiform sys-

→

FIG. 12. Diurnal cycle of the MCS index as shown by fixed-point composites of the index during the dependent study period at 3-h intervals throughout the day. High elevations (i.e., above 750 hPa) are masked out from calculations of the MCS index because of unrepresentative values of the 700-hPa temperature advection.

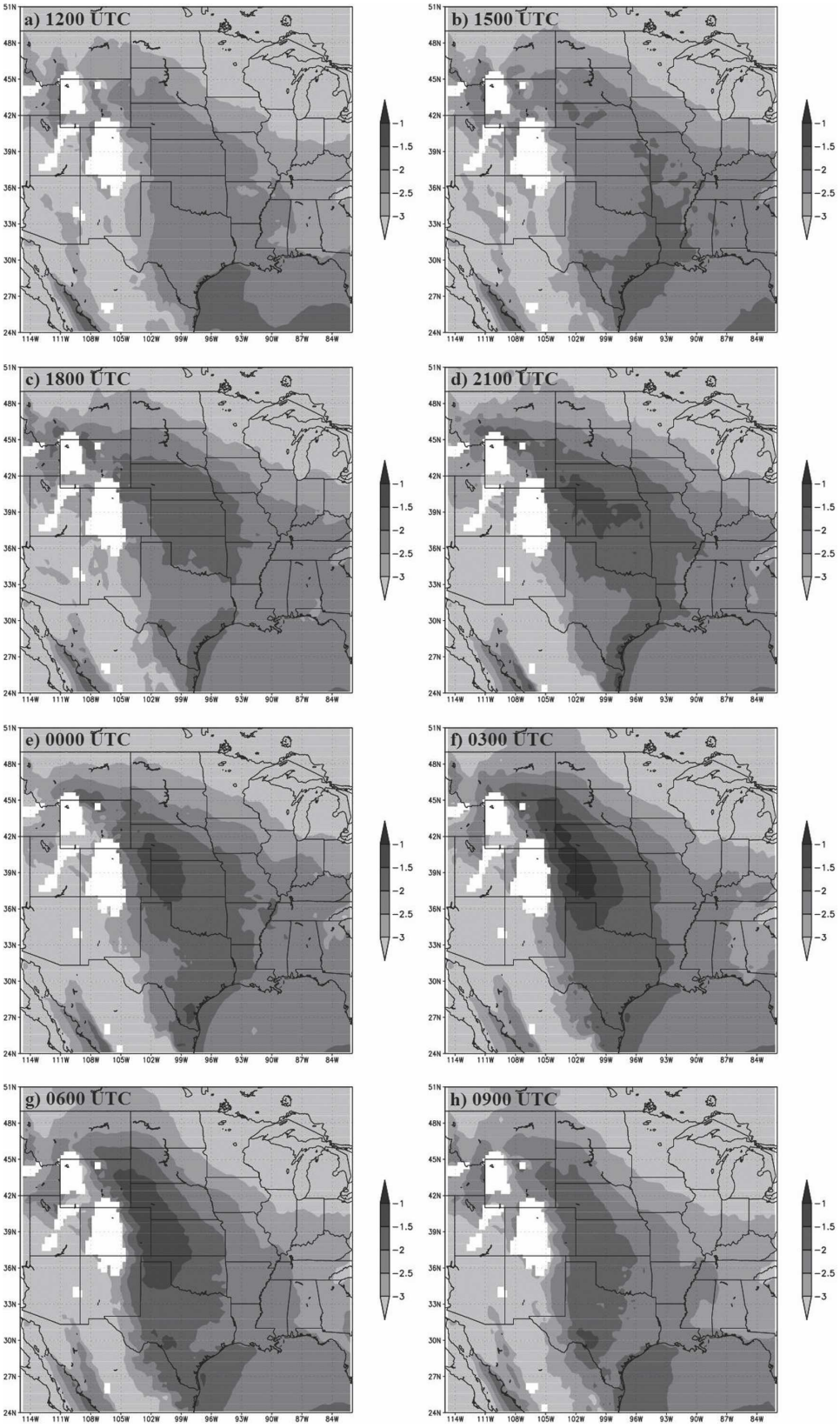
a) 1200 UTC
b) 1500 UTC
c) 1800 UTC
d) 2100 UTC
e) 0000 UTC
f) 0300 UTC
g) 0600 UTC
h) 0900 UTC
51N
48N
45N
42N
39N
36N
33N
30N
27N
24N
114W 111W 108W 105W 102W 99W 96W 93W 90W 87W 84W
−1
−1.5
−2
−2.5
−3

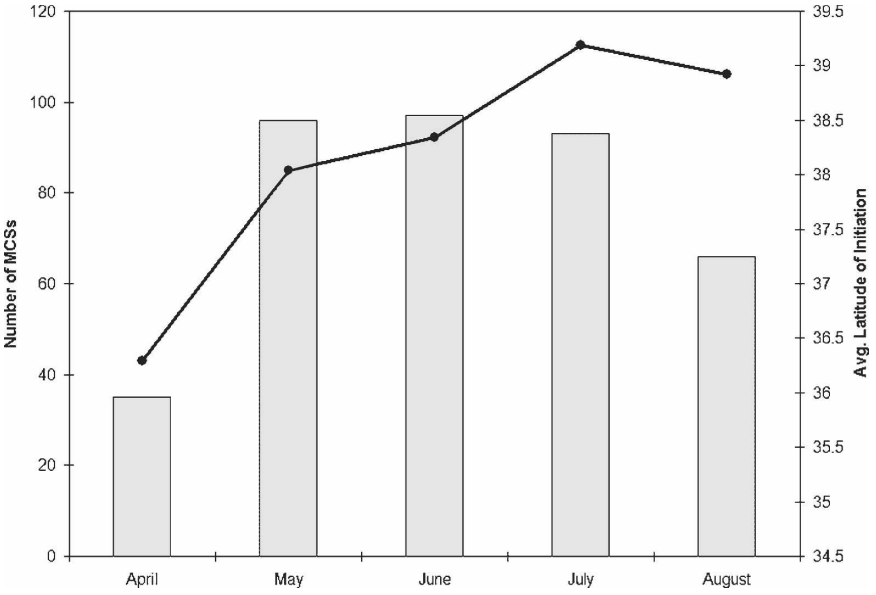

FIG. 13. Distribution (bars) and average latitude of initiation (line) of MCSs by month during the dependent study period.

tem. As the linear MCS moves eastward, it advances into a more unfavorable environment and dissipates.

In the second example, BAMEX forecasters were fairly certain that an MCS would form overnight (i.e., 0000–1200 UTC) on 5 June 2003 in the southern Oklahoma–northern Texas area (Fig. 17a), but they were not sure whether a system would enter the BAMEX domain. Eta Model forecasts of the MCS index (Fig. 17) reveal that favorable conditions for MCS development were not expected within the BAMEX domain overnight on 5 June as far back as the 36-h forecast. The short-term forecasts and 0000 UTC analysis (Fig. 18a) agree on the Texas Panhandle and the area to the south as the primary target for MCS development. Indeed, convection formed and organized in the Texas Panhandle, advancing to the southeast toward central Texas as a bow echo early on 5 June (Fig. 18). In this instance, the MCS index could have been used to reassure forecasters that an MCS would not enter the BAMEX domain.

Overall, these examples illustrate the forecast value provided by the MCS index in determining whether concentrated convection will organize into a coherent system and whether an existing MCS is likely to endure or dissipate. The index will not accurately predict the timing and location of all MCSs and may overestimate MCS development in some instances, especially if a highly concentrated group of thunderstorms does not form. However, the evaluation presented in this section reveals that the MCS index could be a useful tool to forecasters in making decisions about the influence MCSs might have on the immediate and future weather.

7. Summary and conclusions

The precursor environments of hundreds of MCSs and instances of widespread convection were studied in an attempt to gain insight into environmental conditions that favor the development of MCSs from a concentrated group of thunderstorms. An investigation of the initiating mechanisms of these systems revealed that drylines were generally unfavorable locations of MCS development, likely due to a combination of the sparse nature of the convection that develops and unfavorable environmental conditions for supporting convective organization. Stationary and cold fronts were the most common features to generate convection that develops into an MCS. In several instances, however,

→

FIG. 14. Seasonal cycle of the MCS index as shown by fixed-point composites of the index at 0300 UTC during the dependent study period for each month. High elevations (i.e., above 750 hPa) are masked out from calculations of the MCS index because of unrepresentative values of the 700-hPa temperature advection.

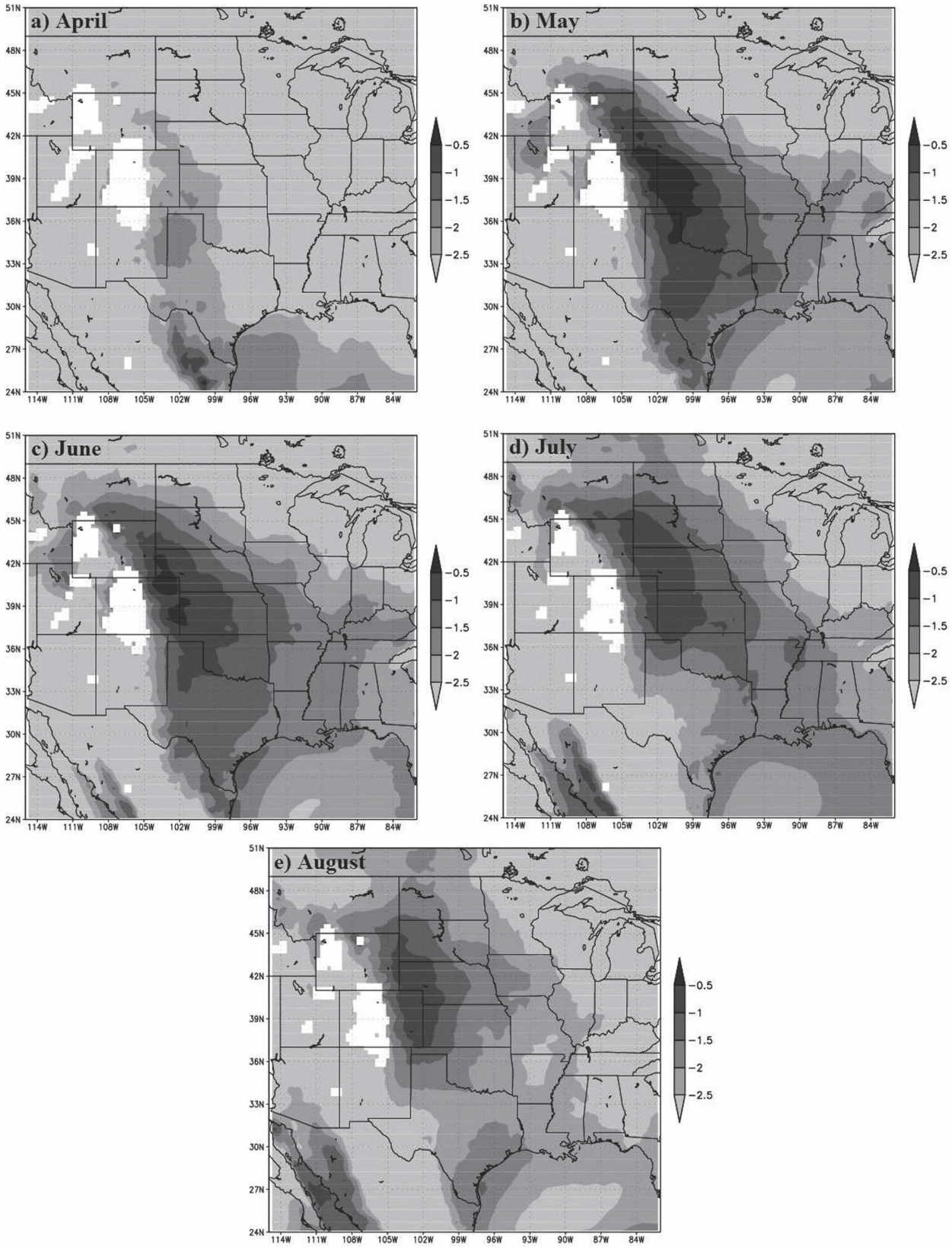
a) April
b) May
c) June
d) July
e) August
51N
48N
45N
42N
39N
36N
33N
30N
27N
24N
114W
111W
108W
105W
102W
99W
96W
93W
90W
87W
84W
−0.5
−1
−1.5
−2
−2.5

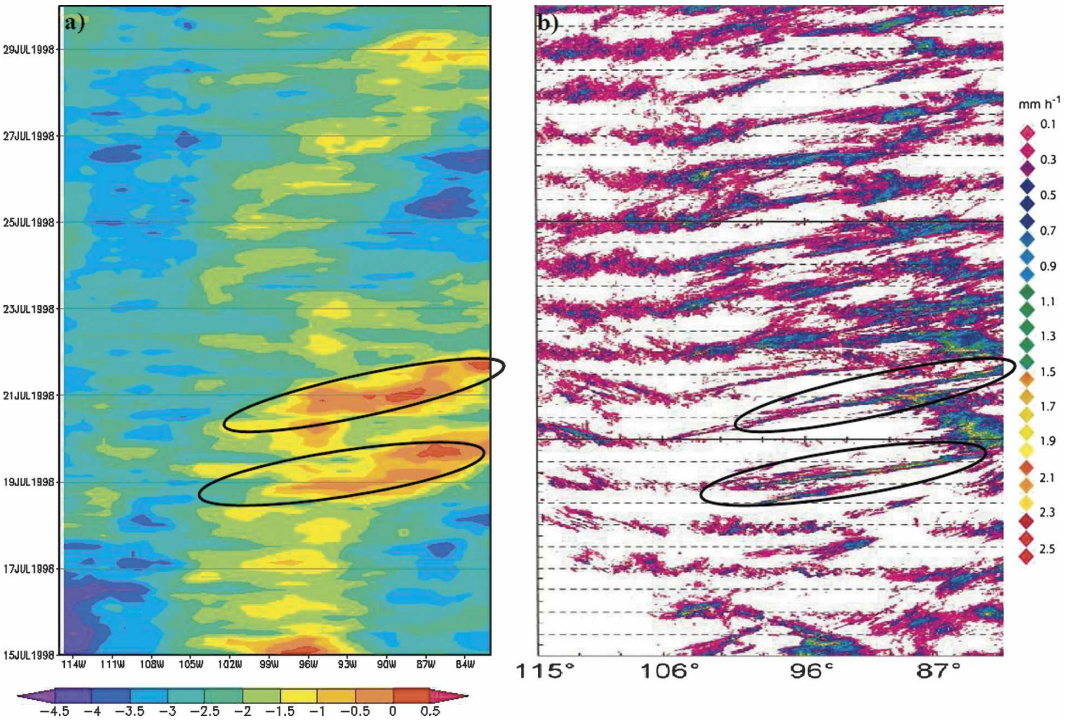

FIG. 15. Hovmöller diagrams for 15–29 Jul 1998 (in UTC) of (a) the MCS index and (b) the radar-derived rain rate (mm h^{-1}) (modified from Carbone et al. 2002). The data are averaged from 30° to 48°N. The elliptical areas encompass examples of precipitation episodes and the corresponding values of the MCS index.

concentrated convection developed along a frontal boundary that did not evolve into an MCS. Similarly, widespread convection was found to typically form in a region of higher midlevel PV than MCSs. These results suggest that even if some feature is present to enhance the initiation of convection, the environment still often needs to lend additional support for the development and organization of long-lived convective systems.

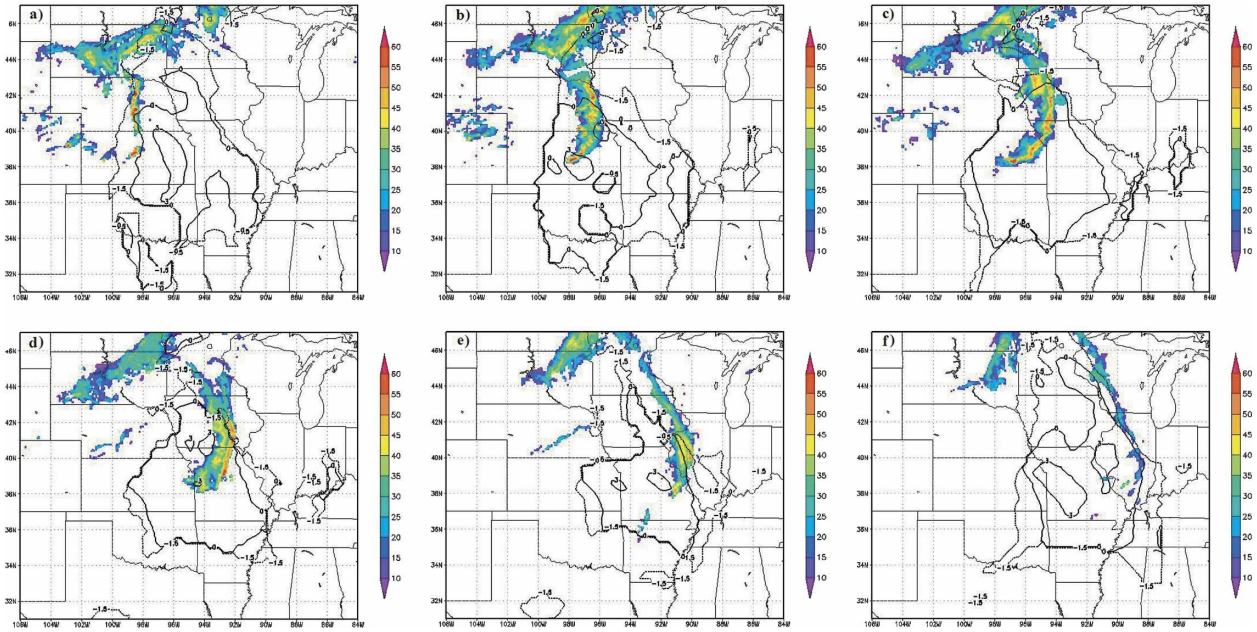

FIG. 16. Radar reflectivity (shaded) and MCS index (contoured at −1.5, 0, and 3) on 12 May 1998. The images are from (a) 0000, (b) 0300, (c) 0600, (d) 0900, (e) 1200, and (f) 1500 UTC 12 May 1998.

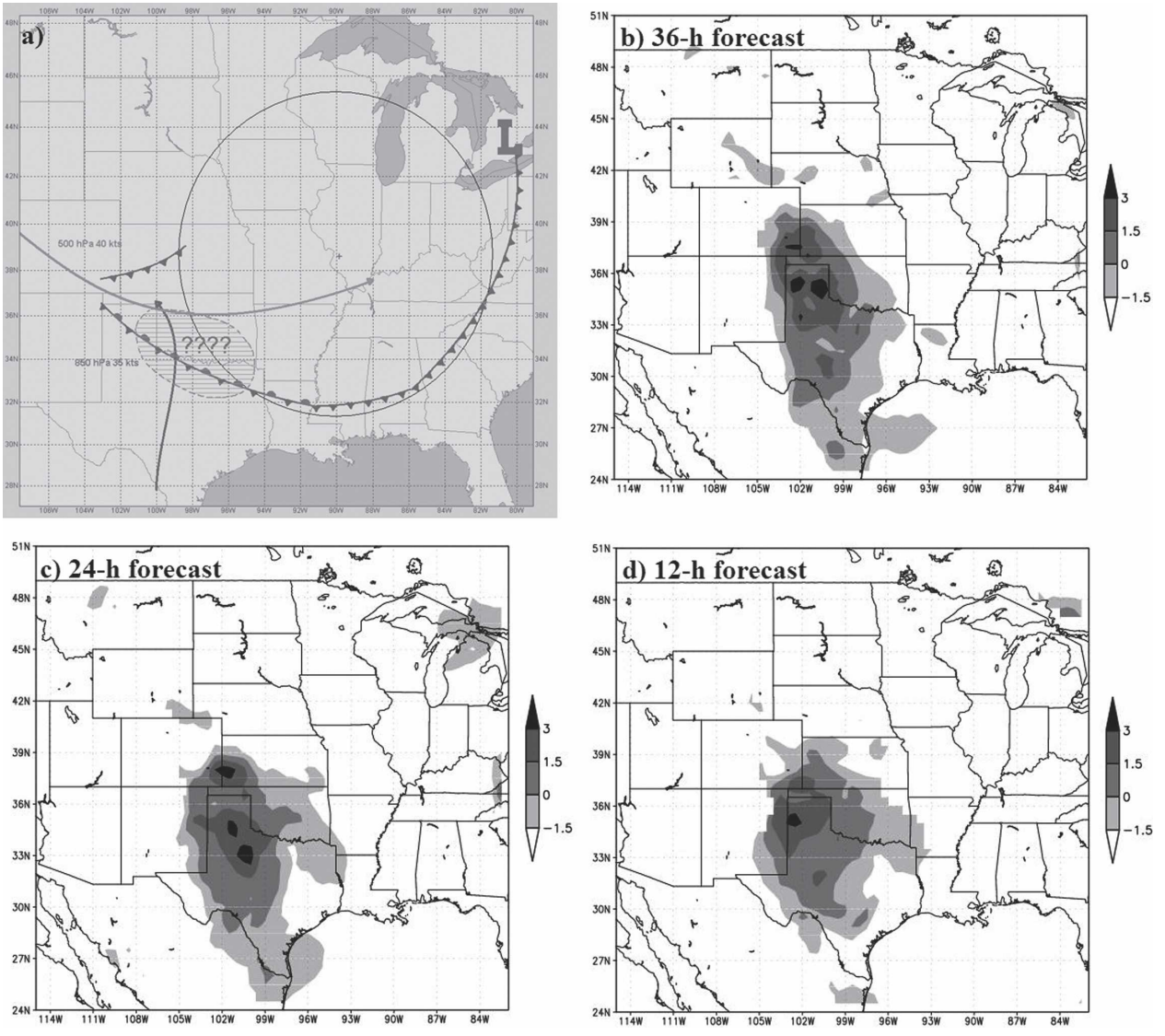

FIG. 17. MCS forecasts made for 5 Jun 2003: (a) BAMEX forecast made at 2245 UTC 4 Jun 2003 valid for 0000–1200 UTC 5 Jun, and (b) 36-, (c) 24-, and (d) 12-h Eta Model forecasts of the MCS index valid at 0000 UTC 5 Jun 2003. In (a), the hatched region identifies the probable location of MCS development, and the circle identifies the BAMEX domain centered on St. Louis.

To identify environmental features that aid in convective development and organization, the environments of MCSs and widespread convection were analyzed and statistically significant differences were found between these conditions. Low-level warm air advection was much larger on average prior to MCS development than for unorganized convection. Wind speeds were also much stronger for the MCS precursor environments leading to stronger vertical wind shear through the lower troposphere. In addition, the environments that supported MCS development were typically more unstable than the environments of widespread convection. The MCS-relative composites also revealed good correspondence between the maximum of each of these parameters and the average location of MCS initiation.

Based on these results, 700-hPa temperature advection, 0–3-km shear, and LI were selected to be part of an index used to forecast MCS development. Low-level warm air advection and ambient shear act to enhance lifting that allows the rising air to tap into convective instability, promoting the development of an organized convective system. These parameters form the basis of the MCS index by providing a likelihood that the atmosphere will support the development of an MCS from a group of thunderstorms.

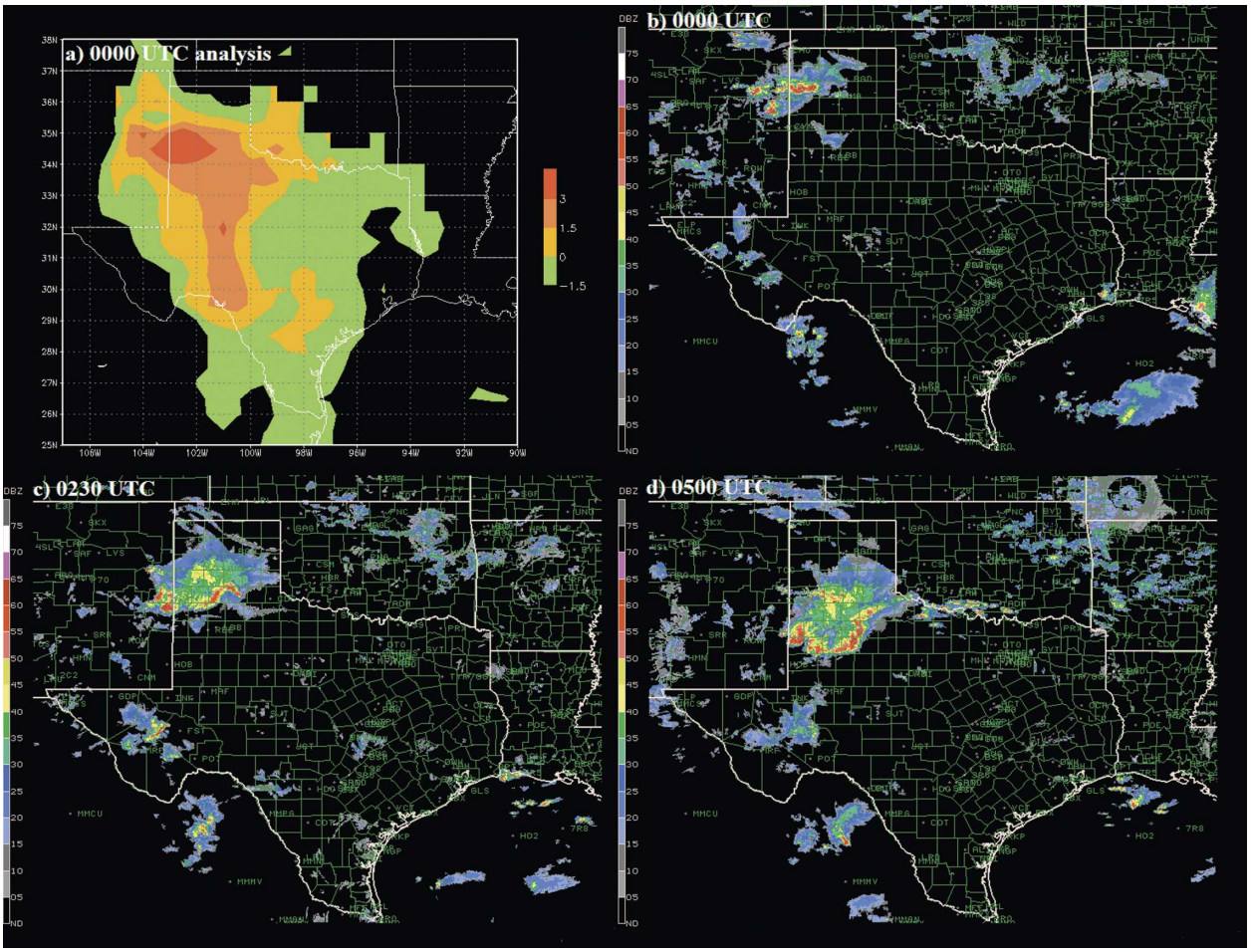

FIG. 18. Eta analysis of the MCS index at (a) 0000 UTC 5 Jun 2003 and composite radar reflectivity at (b) 0000, (c) 0230, and (d) 0500 UTC 5 Jun 2003.

The resulting MCS index demonstrated significant accuracy in forecasting MCSs during the dependent study period and during BAMEX, an independent convective season. The greatest utility of the MCS index is in identifying whether existing convection will merge and undergo upscale growth into an MCS. In addition, the index provides an indication of whether the environment is favorable for supporting an existing MCS. In an averaged sense, the MCS index exhibits features similar to MCS characteristics, including the diurnal and seasonal cycles. The MCS index also typically shows good agreement with precipitation episodes even during weakly forced midsummer conditions.

Overall, the MCS index should be very helpful to forecasters in predicting the influence MCSs might have on the weather in a given area, especially considering the lack of formal forecast methods currently available (Ziegler 2000). As long as the MCS index is used in conjunction with other information, such as the location and timing of convective initiation, it should lead to improved, yet imperfect, forecasts. Future studies of the MCS index involving an analysis of its performance in real-time, global applications and a comparison with independent objective statistical analyses are suggested to lead to possible modifications and improvements of the existing index. Undoubtedly, progress in the area of MCS predictability will continue as insight gained from this study will stimulate more studies to further our understanding of MCSs.

Acknowledgments. The authors thank C. Doswell and two anonymous reviewers for comments and suggestions that helped to improve this manuscript. The Global Hydrology Resource Center at the Global Hydrology and Climate Center, National Climatic Data Center, and National Center for Atmospheric Research–University Corporation for Atmospheric Research provided access to data that made this study

possible. This research was supported by National Science Foundation (NSF) Graduate Fellowship DGE-0234615 and NSF Grant ATM-0324324.

REFERENCES

Anderson, C. J., and R. W. Arritt, 1998: Mesoscale convective complexes and persistent elongated convective systems over the United States during 1992 and 1993. *Mon. Wea. Rev.,* **126,** 578–599.

Ashley, W. S., T. L. Mote, P. G. Dixon, S. L. Trotter, E. J. Powell, J. D. Durkee, and A. J. Grundstein, 2003: Distribution of mesoscale convective complex rainfall in the United States. *Mon. Wea. Rev.,* **131,** 3003–3017.

Augustine, J. A., and K. W. Howard, 1988: Mesoscale convective complexes over the United States during 1985. *Mon. Wea. Rev.,* **116,** 685–700.

——, and F. Caracena, 1994: Lower-tropospheric precursors to nocturnal MCS development over the central United States. *Wea. Forecasting,* **9,** 116–135.

Barnes, S. L., 1964: A technique for maximizing details in numerical weather map analysis. *J. Appl. Meteor.,* **3,** 396–409.

Carbone, R. E., J. D. Tuttle, D. A. Ahijevich, and S. B. Trier, 2002: Inferences of predictability associated with warm season precipitation episodes. *J. Atmos. Sci.,* **59,** 2033–2056.

Cotton, W. R., and R. A. Anthes, 1989: *Storm and Cloud Dynamics*. Academic Press, 883 pp.

——, R. L. George, P. J. Wetzel, and R. L. McAnelly, 1983: A long-lived mesoscale convective complex. Part I: The mountain-generated component. *Mon. Wea. Rev.,* **110,** 1893–1918.

——, M. S. Lin, R. L. McAnelly, and C. J. Tremback, 1989: A composite model of mesoscale convective complexes. *Mon. Wea. Rev.,* **117,** 765–783.

Davis, C., and Coauthors, 2004: The bow echo and MCV experiment: Observations and opportunities. *Bull. Amer. Meteor. Soc.,* **85,** 1075–1093.

Doswell, C. A., III, 1977: Obtaining meteorologically significant surface divergence fields through the filtering property of objective analysis. *Mon. Wea. Rev.,* **105,** 885–892.

——, and J. A. Flueck, 1989: Forecasting and verifying in a field research project: DOPLIGHT '87. *Wea. Forecasting,* **4,** 97–109.

——, R. Davies-Jones, and D. L. Keller, 1990: On summary measures of skill in rare event forecasting based on contingency tables. *Wea. Forecasting,* **5,** 576–585.

Douglas, M. W., R. A. Maddox, K. Howard, and S. Reyes, 1993: The Mexican monsoon. *J. Climate,* **6,** 1665–1677.

Fritsch, J. M., R. J. Kane, and C. R. Chelius, 1986: The contribution of mesoscale convective weather systems to the warm-season precipitation in the United States. *J. Climate Appl. Meteor.,* **25,** 1333–1345.

——, J. D. Murphy, and J. S. Kain, 1994: Warm core vortex amplification over land. *J. Atmos. Sci.,* **51,** 1780–1807.

——, and Coauthors, 1998: Quantitative precipitation forecasting: Report of the Eighth Prospectus Development Team, U.S. Weather Research Program. *Bull. Amer. Meteor. Soc.,* **79,** 285–299.

Hertenstein, R. F. A., and W. H. Schubert, 1991: Potential vorticity anomalies associated with squall lines. *Mon. Wea. Rev.,* **119,** 1663–1672.

Houze, R. A., Jr., B. F. Smull, and P. Dodge, 1990: Mesoscale organization of springtime rainstorms in Oklahoma. *Mon. Wea. Rev.,* **118,** 613–654.

Jincai, D., C. A. Doswell III, D. W. Burgess, M. P. Foster, and M. L. Branick, 1992: Verification of mesoscale forecasts made during MAP '88 and MAP '89. *Wea. Forecasting,* **7,** 468–479.

Jirak, I. L., W. R. Cotton, and R. L. McAnelly, 2003: Satellite and radar survey of mesoscale convective system development. *Mon. Wea. Rev.,* **131,** 2428–2449.

Johns, R. H., and C. A. Doswell III, 1992: Severe local storms forecasting. *Wea. Forecasting,* **7,** 588–612.

Johnson, R. H., S. Chen, and J. J. Toth, 1989: Circulations associated with a mature-to-decaying mesoscale convective system. Part I: Surface features—Heat bursts and mesolow development. *Mon. Wea. Rev.,* **117,** 942–959.

Laing, A. G., and J. M. Fritsch, 1997: The global population of mesoscale convective complexes. *Quart. J. Roy. Meteor. Soc.,* **123,** 389–405.

——, and ——, 2000: The large-scale environments of the global populations of mesoscale convective complexes. *Mon. Wea. Rev.,* **128,** 2756–2776.

Maddox, R. A., 1980: Mesoscale convective complexes. *Bull. Amer. Meteor. Soc.,* **61,** 1374–1387.

——, 1983: Large-scale meteorological conditions associated with midlatitude, mesoscale convective complexes. *Mon. Wea. Rev.,* **111,** 126–140.

——, and C. A. Doswell III, 1982: An examination of jet stream configurations, 500 mb vorticity advection and low-level thermal advection patterns during extended periods of intense convection. *Mon. Wea. Rev.,* **110,** 184–197.

McAnelly, R. L., and W. R. Cotton, 1986: Meso-β scale characteristics of an episode of meso-α scale convective complexes. *Mon. Wea. Rev.,* **114,** 1740–1770.

McNulty, R. P., 1995: Severe and convective weather: A central region forecasting challenge. *Wea. Forecasting,* **10,** 187–202.

Mesinger, F., and Coauthors, 2006: North American Regional Reanalysis. *Bull. Amer. Meteor. Soc.,* **87,** 343–360.

Olson, D. A., N. W. Junker, and B. Korty, 1995: An evaluation of three decades of quantitative precipitation forecasting at the Meteorological Operations Division of the National Meteorological Center. *Wea. Forecasting,* **10,** 498–511.

Olsson, P. Q., and W. R. Cotton, 1997: Balanced and unbalanced circulations in a primitive equation simulation of a midlatitude MCC. Part I: The numerical simulation. *J. Atmos. Sci.,* **54,** 457–478.

Parker, M. D., and R. H. Johnson, 2000: Organizational modes of midlatitude mesoscale convective systems. *Mon. Wea. Rev.,* **128,** 3413–3436.

Rasmussen, E. N., 2003: Refined supercell and tornado forecast parameters. *Wea. Forecasting,* **18,** 530–535.

——, and D. O. Blanchard, 1998: A baseline climatology of sounding-derived supercell and tornado forecast parameters. *Wea. Forecasting,* **13,** 1148–1164.

Raymond, D. J., and H. Jiang, 1990: A theory for long-lived mesoscale convective systems. *J. Atmos. Sci.,* **47,** 3067–3077.

Rhea, J. O., 1966: A study of thunderstorm formation along drylines. *J. Appl. Meteor.,* **5,** 58–63.

Rotunno, R., J. B. Klemp, and M. L. Weisman, 1988: A theory for strong, long-lived squall lines. *J. Atmos. Sci.,* **45,** 463–485.

Sanders, F., and C. A. Doswell III, 1995: A case for detailed surface analysis. *Bull. Amer. Meteor. Soc.,* **76,** 505–521.

Smull, B. F., and J. A. Augustine, 1993: Multiscale analysis of a

mature mesoscale convective complex. *Mon. Wea. Rev.,* **121,** 103–132.

Stensrud, D. J., and J. M. Fritsch, 1994: Mesoscale convective systems on weakly forced large-scale environments. Part II: Generation of a mesoscale initial condition. *Mon. Wea. Rev.,* **122,** 2068–2083.

Trier, S. B., and D. B. Parsons, 1993: Evolution of environmental conditions preceding the development of a nocturnal mesoscale convective complex. *Mon. Wea. Rev.,* **121,** 1078–1098.

Uccellini, L. W., and D. R. Johnson, 1979: The coupling of upper and lower tropospheric jet streaks and implications for the development of severe convective storms. *Mon. Wea. Rev.,* **107,** 682–703.

Weisman, M. L., 1992: The role of convectively generated rear-inflow jets in the evolution of mesoconvective systems. *J. Atmos. Sci.,* **49,** 1826–1847.

——, and J. B. Klemp, 1982: The dependence of numerically simulated convective storms on vertical wind shear and buoyancy. *Mon. Wea. Rev.,* **110,** 504–520.

——, and ——, 1984: The structure and classification of numerically simulated convective storms in directionally varying wind shears. *Mon. Wea. Rev.,* **112,** 2479–2498.

——, and R. Rotunno, 2004: "A theory for strong long-lived squall lines" revisited. *J. Atmos. Sci.,* **61,** 361–382.

Wilks, D. S., 1995: *Statistical Methods in the Atmospheric Sciences*. Academic Press, 464 pp.

Ziegler, C. L., 2000: Issues in forecasting mesoscale convective systems: An observational and modeling perspective. *Storms,* R. Pielke Jr. and R. Pielke Sr., Eds., Routledge Press, 26–42.